UCL Université catholique de Louvain

Faculté des Sciences Appliquées

Département des sciences des matériaux et des procédés

Unité de physico-chimie et d'ingénierie des matériaux (PCIM)

On the Physics and Mechanics of Phase Transformations in TRIP-Assisted Multiphase Steels

Pascal Jacques

Promoteur : F. Delannay

Dissertation présentée en vue de l'obtention du grade de Docteur en Sciences Appliquées

Louvain-la-Neuve, December 1998

In the Beginning
Was Austenite...
And then,
Austenite transformed to Martensite...

G. Krauss, ICOMAT98,
Bariloche, Argentina

Peut-être y a-t-il d'autres connaissances à acquérir, d'autres interrogations à poser aujourd'hui, en partant, non de ce que d'autres ont su, mais de ce qu'ils ont ignoré.

S. Moscovici

Enrouler le monde autour de nos doigts
Comme un fil ou un ruban dont joue une femme qui rêve à sa fenêtre.

F. Pessoa, "Fragments d'un
voyage immobile"

Remerciements

Pourrait-on imaginer une thèse sans remerciements ? Pour moi, certainement pas ! Elle est fausse l'image du chercheur isolé, perdu au fin fond de son laboratoire. Une thèse, c'est d'abord une aventure humaine, une histoire de grandes joies ou de déceptions, de moments intenses ou paisibles, mais toujours partagés. Une thèse, c'est une histoire de collaborations, d'échanges, de longues conversations où l'on reconstruit le monde, ou plutôt ses mondes. C'est pour toutes ces petites et grandes choses que je veux remercier mes collaborateurs(-trices), tous ces ami(e)s dont j'ai croisé la route et sans qui, arriver à écrire ces quelques mots eût été chose impossible.

Tout d'abord, mes remerciements les plus sincères vont aux membres du jury, à Monsieur le Président, le Professeur J.-P. Issi, au Professeur Y. Houbaert (de la R.U. Gent), à Monsieur V. Leroy (du C.R.M.), au Professeur E. Aernoudt (de la K.U. Leuven, membre du comité d'encadrement), au Professeur J. Ladrière (membre du comité d'encadrement) et à Monsieur le Professeur F. Delannay (promoteur) pour leur lecture attentive du manuscrit et pour la discussion pertinente et enrichissante de la pré-défense.

Je tiens à remercier tout particulièrement l'Université catholique de Louvain, le centre R&D du Groupe Cockerill-Sambre et la Région Wallonne pour avoir financé cette recherche doctorale et m'avoir permis d'arriver au terme de cette thèse.

Pour arriver au terme d'une thèse, il faut plus que la possibilité de l'accomplir; il faut des guides qui jalonnent votre périple et vous aident dans votre ascension. Monsieur Delannay, cher Francis, vous êtes un de ces guides, toujours à la recherche de l'équilibre de chacun avec cette petite touche en plus, ce souci constant de laisser le libre choix. Il y a quatre ans, nous nous sommes lancés dans cette thèse, un défi comme je les aime et que sans nul doute vous appréciez tout autant. Aujourd'hui, je vous dis de tout cœur merci pour en avoir permis l'épanouissement avec à tout instant la même gentillesse et le même intérêt.

D'autres guides, je les ai trouvés sur les hauteurs de Liège, au centre R&D du Groupe Cockerill-Sambre. Monsieur Renard, Monsieur Weymeersch, merci à vous pour votre confiance et votre aide. Me rendre à RDCS a toujours été un réel plaisir, et je suis très fier d'avoir pu partager avec vous et vos collaborateurs de nombreuses réflexions sur ce

matériau fascinant qu'est l'acier. Cher Philippe, quelle épopée entre notre première réunion où j'apprenais ce qu'était l'acier, le vrai, et cette conférence mémorable à Pittsburgh ! Merci pour le temps (une denrée rare...) et l'énergie que tu as investis dans ce projet. Nos longues discussions lui ont donné une ramification 'appliquée' assez prometteuse, une motivation supplémentaire. A RDCS, j'ai aussi découvert les joies de la métallographie. Ah ! Quel accueil chaleureux chaque fois renouvelé ! Eugène, Sylvano, Daniel et tous les autres, merci pour votre aide et vos petits trucs. Fausto, nous faisions vraiment une équipe de lamineurs fous. Ça n'a pas été facile (d'ailleurs, les armoires derrière le laminoir s'en souviennent encore...), mais on y est arrivé. Un tout grand merci pour ton aide. Klaus, ton acharnement et ton investissement scientifique étaient phénoménaux. Merci pour tout. Enfin, merci à tous ceux et celles qui m'ont aidé à un moment ou à un autre.

Etienne, cher ami, on a connu les mêmes galères mais aussi et surtout les mêmes succès. Face à la complexité (reconnue – ce sont les autres qui le disent) des aciers, il fallait bien une équipe de choc renouvelant la déjà vieille amitié franco-belge. Quelle joie et quelle efficacité dans cette collaboration ! J'en veux pour preuve le succès du *team* KUL-UCL en Patagonie. Merci pour ton aide, tes conseils, mais pas pour ton analyse de certains faits footballistiques.

Xavier, Anne, Tanguy, Quentin, je vous dois une fière chandelle ! Vous conseiller dans votre travail de fin d'études a été pour moi une véritable joie et une expérience enrichissante. Je l'ai fait avec passion et j'espère que j'ai pu vous en transmettre un peu, comme d'autres l'avaient fait avec moi en leur temps. Merci pour tout.

Et puis, il y a le PCIM !
Il y règne une ambiance amicale, un peu familiale, propice à toutes ces petites choses apparemment insignifiantes mais que l'on n'oubliera jamais vraiment. Merci à vous tous pour cette richesse humaine et scientifique, pour ces moments inoubliables. René, ta jeunesse d'esprit est éternelle et ton aide, indispensable; tes 'ghislaineries' m'ont été très précieuses. Marc, que dire sinon que tu es (un peu soupe au lait ... allez, c'est une blague) vraiment exceptionnel. Il ne faut pas longtemps pour s'en convaincre et très vite, on ne peut plus se passer de ton savoir-faire... et de ton amitié. A vous deux, vous faites aussi un repère indispensable pour l'accomplissement de cette thèse. Merci, Monsieur Streydio, pour votre franc-parler et votre dynamisme; Laurence, pour cette attention toute maternelle... et pour les séances de TEM (improvisées en pleine rédaction, histoire de souffler un peu). Merci à ces anciens d'une certaine expédition... Christophe, Hannibal, *notre* français, pour ta gentillesse et ta méthode de travail ('the well-known CC Method'); François, Looping, pour tes aphorismes teintés de bons sens; Thomas, Futé, pour ton aide,

la clarté de tes explications et ton vin. Merci, Catherine, pour ta simplicité, ton naturel (souvent rougeâtre) et ta bonne humeur; Jean-Yves, pour ces longues discussions, parfois techniques, ou philosophiques, voire musicales, pour ta créativité à la démesure de ton ordre; Albert, pour toutes ces informations dûment transmises; Emile, pour ton dévouement et ta patience. Enfin, merci aux jeunes, Anne, Delphine, Vincent et aux petits jeunes, Thierry, Quentin et Stéphane (n'oubliez pas de vous entraîner aux flèches ...), Sophie, pour nous rappeler, aux plus anciens, qu'il est temps de chercher d'autres aventures. Tous, cultivez et faites perdurer cet esprit *pcimiens*...

Merci à mes parents, sœurs, frère et toute ma famille pour m'avoir soutenu (souvent supporté) et aidé tout ce temps. Enfin, merci à tous ces compañeros et autres petites personnes dont j'ai croisé la route. Dans l'ombre, vous avez aussi votre part de responsabilité dans l'accomplissement de ce projet...

Table of Contents

Introduction

Although sometimes considered as an 'old' material, steel remains the most widely used metallic alloy[1] and a subject of intense research. More than one century of research on the physical metallurgy of steels[2] has not yet allowed a thorough understanding of the physics governing the processing and properties of this 'common' material. The versatility of steel has its origin in the different allotropic forms of iron, in the many mechanisms by which phase transformations can develop and in the solubility of carbon and substitutional solutes in these phases. As a consequence, steels certainly constitute the most complex group of alloys for large scale use, exhibiting an incredibly rich variety of microstructures and therefore, of properties which can be exploited by industry. The development of a new steel is a kind of a modern quest for the 'Philosopher's Stone', a stone that would allow turning base iron into steel with improved properties.

The automotive industry is certainly one of the key sectors in which continuous improvement of the steel properties is insistently requested. With respect to emerging materials such as aluminium or composites, steel will keep its place as the first material for vehicles if it meets the new requirements of the automotive industry. For some years now, a primary objective of development is the reduction of weight in vehicles in order to reduce fuel consumption and thus emission of greenhouse gas. The recent Global Warming Treaty of Kyoto reveals the extent and importance of this requirement. Furthermore, more stringent requirements for safety and crashworthiness are imposed by the governments and

[1] The production of steel in the world is predicted to increase to about 1 000 million tonnes by the year 2000!

[2] Names such as H.C. Sorby, A. Martens or L.J. Troost are associated with the birth of metallography and the first steps in the understanding of the hardening processes of steels at the end of the 19th century (see for example: C.S. Smith: *Martensite*, G.B. Olson and W.S. Owen ed, ASM, 1992, pp. 11-21).

standards associations. The recent Ultra Light Steel Auto Body (ULSAB) project, which has brought together on a world-wide scale members of the steelmaking industry and automotive industry, demonstrates the possibilities of lightweight automobile construction with modern steels and processes by attaining a weight saving of 25%. Within the scope of the ULSAB project, high-strength steels were largely used to a great advantage.

The new challenge for optimising vehicle structures for weight is to develop steels with enhanced strength without compromising formability. The ***TRIP-assisted multiphase steels*** meet this requirement. For a decade now, numerous studies have shown that TRIP-assisted multiphase steels are particularly remarkable among the high-strength steels since they do not seem to follow the traditional axiom of materials engineering dictating that ductility goes down as strength goes up. However, the steels studied up to now contain a high level of silicon which is too high as to be compatible with industrial practice. This feature constitutes the major drawback for the large scale developments of these steels. The need for high-strength formable steels with a reduced silicon content therefore seems necessary.

Beside these applied aspects, a study of TRIP-assisted multiphase steels also aims at a better understanding of the physical principles underlying this new material. The unique strength-ductility balance of TRIP-assisted multiphase steels emerges from (i) a complex microstructure associating ferrite, bainite, retained austenite and martensite, which is generated at the end of a specific heat-treatment scheme; (ii) the exploitation of a particular mechanism of deformation, i.e. the mechanically-induced martensitic transformation of metastable austenite (the TRIP effect). As a matter of fact, the physics underlying the phase transformations or the mechanical behaviour of these steels is not fully understood. The formation of bainite and martensite during either thermal processing or mechanical testing has still to be thoroughly elucidated. A description of the mechanical properties of the TRIP-assisted multiphase steels, accounting for the composite nature of their microstructure as well as for the role of the TRIP effect is also of primary importance.

The subject of this thesis is twofold:

(i) to contribute to the understanding of the phase transformations and mechanical properties of TRIP-assisted multiphase steels;

(ii) to show to what extent a new TRIP-assisted multiphase steel with a reduced silicon content could meet the performance requirements for high-strength formable steels.

Each chapter will be devoted to enlightening a specific aspect of the behaviour of the TRIP-assisted multiphase steels during either thermal processing or mechanical testing. In each case, the correlations between *Processing, Microstructure* and *Properties* will be established. Furthermore, the different investigations carried out in this thesis will aim at comparing what can be called a *conventional* high silicon TRIP-assisted multiphase steel with a newly proposed low silicon TRIP-assisted multiphase steel.

The outline of the thesis follows the logical evolution from processing to mechanical testing:

Chapter I reviews the main literature results concerning various steel families to which TRIP-assisted multiphase steels can be related. This chapter thus provides a first insight into the unique properties of these steels. Some relevant features of the Dual Phase steels are presented. The TRIP effect is briefly described as well as some features of the bainite transformation that can bring about the stabilisation of austenite.

Chapter II describes the different steels investigated in this thesis as well as the experimental procedures designed and used in order to enlighten the factors governing the phase transformations and mechanical properties of TRIP-assisted multiphase steels.

Chapter III is devoted to the investigation of the phase transformations occurring during the thermal processing of cold-rolled TRIP-assisted multiphase steels, with particular attention to the bainite transformation of intercritical austenite. The influence of the silicon content and of the temperature of bainitic tempering is highlighted. The kinetics of bainite transformation during thermal processing is explained on the basis of the morphological characteristics of intercritical austenite.

Chapter IV deals with the correlations existing in TRIP-assisted multiphase steels between the uniaxial tensile properties and some features of the microstructure. The relationship between (i) the formation and transformation of austenite during thermal processing, (ii) the generated microstructures and (iii) the resulting mechanical properties are clearly demonstrated. Beside the TRIP effect, the role of other strengthening mechanisms is also enlightened.

Chapter V deals with the characterisation of the mechanical stability of retained austenite in TRIP-assisted multiphase steels and the efficiency of the TRIP effect at room temperature. The influences of chemical composition and heat-treatment parameters on the stability of retained austenite are elucidated. The effect of the other phases surrounding

austenite is also established. The use of the acoustic emission technique in order to characterise the transformation rate of austenite during uniaxial tensile testing of TRIP-assisted multiphase steels is demonstrated.

Chapter VI is devoted to the characterisation of the mechanical stability of retained austenite by considering the temperature dependence of tensile properties. A reversal of flow stresses at small strain offsets (as well as of other properties) corresponding to M_s^{σ} is experimentally defined. This temperature dependence of the mechanical properties is related to the intrinsic mechanical stability of retained austenite independently of the influence of the surrounding phases.

Chapter VII deals with the characterisation of the damage and fracture resistance of the TRIP-assisted multiphase steels. The transformation and damage of notched plates is studied by fracture toughness testing using DENT specimens and by numerical simulations. This study reveals the parameters of the microstructure dictating the fracture resistance of this type of steel. Furthermore, a phenomenological energetic criterion for the mechanically-induced martensitic transformation is proposed.

The conclusion summarises the main results of the thesis and suggests some prospects.

Chapter I

From Dual Phase Steels to TRIP-Assisted Multiphase Steels

1. Introduction

For a decade now, studies dealing with new high-strength low alloy steels exhibiting enhanced formability attract a large interest in the literature. These studies are principally motivated by the pressure of the automotive industry which is looking for new materials with an improved strength-ductility balance. These materials should thus meet in a more effective way the objectives of reduction of car consumption by weight saving. They do also improve safety and crashworthiness. As sketched in figure 1.1, these new steel grades are called ***TRIP-assisted multiphase steels***. Their appellation thus recalls the 2 physical origins of their exceptional mechanical properties, i.e. the multiphase nature of their microstructure and the possibility of a TRIP effect (i.e. mechanically-induced martensitic transformation of metastable retained austenite). The word 'assisted' (which is often forgotten in the literature) means that these 2 features interact and influence each other. TRIP-assisted multiphase steels can be considered as historically deriving from various previously developed iron-based alloys. This chapter intends to show how the

characteristics of TRIP-assisted multiphase steels can be logically related to these previous steel families.

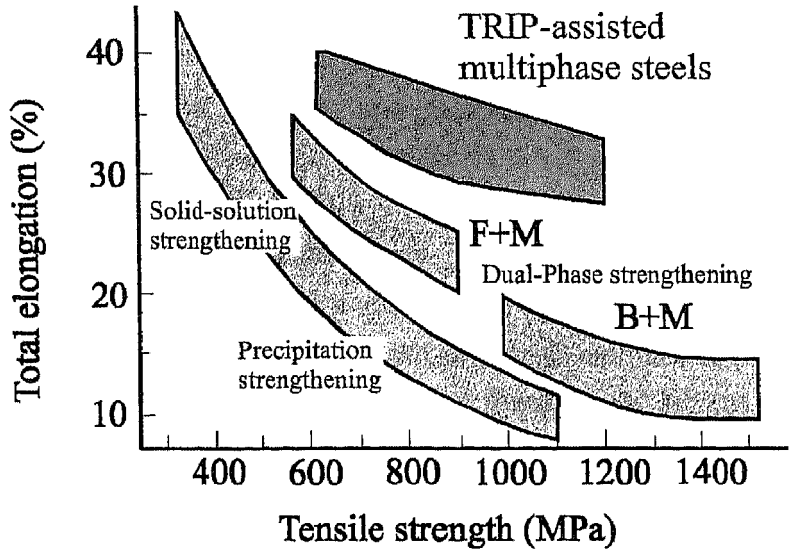

Figure 1.1: Typical combinations of strength and ductility obtained with conventional strengthening mechanisms of low alloy steels.

First of all, the TRIP-assisted multiphase steels present a ***multiphase microstructure***. They are thus clearly related to the ***Dual-Phase steels*** thoroughly studied since the end of the 1970s. Like the Dual-Phase steels, the TRIP-assisted multiphase steels are obtained through an improved control of the thermal or thermomechanical processing of low and medium carbon steels. Furthermore, TRIP-assisted multiphase steels make use of the ***TRIP effect***. They are thus related to the highly alloyed ***fully austenitic steels*** for which it had been shown that mechanically triggered martensitic transformation can contribute very effectively to the deformation mechanism. In these fully austenitic steels, austenite could be retained thanks to high levels of expensive alloying elements. The question was therefore to find out how austenite could be retained with sufficient stability in a low alloy steel. As Dual-Phase heat-treatment does not yield to such a stabilisation, ***bainite transformation*** revealed to be a very powerful means which could lead to large amounts of retained austenite when particular conditions are fulfilled.

The present chapter aims at reviewing the principal literature results concerning the Dual-Phase steels, i.e. concerning their chemical composition, mechanical properties and underlying strengthening mechanisms. A short insight about the TRIP effect will be presented. Retained austenite with improved stability can be found in high strength bainitic steels. The mechanism by which bainite transformation can bring about large amounts of retained austenite will therefore be enlightened. The combined effects of these different parameters in TRIP-assisted multiphase steels will finally be summarised.

2. Emergence of Dual-Phase steels

2.1. A new process practice

Thermomechanical processing of low- and medium-carbon steels commonly involves cooling from above the upper critical temperature (A_3) where only austenite is stable [Davi79, Matl82]. Proper control of alloy composition and cooling rate allows obtaining various desirable combinations of microstructure and properties. For example, low carbon steel sheets used in applications where good ductility is required are cooled at such a rate that microstructures consist primarily of ferrite and small amounts of pearlite or carbides. Microalloying and/or controlled hot-rolling have dramatically increased the strength of low-carbon steel sheets by refining grain size in what is referred to as 'High-Strength Low Alloy' (HSLA) steels. The microstructure of HSLA steels still largely consists of ferrite with some pearlite.

With the Dual-Phase steels, other processing approaches than those which produce exclusively either ferrite/pearlite *or* martensite (in the case of ultra-strength steels) microstructures have been developed. These new approaches result in microstructures consisting of ferrite *and* martensite, therefore combining in the same microstructure phases with largely different mechanical properties in order to give rise to a synergetic composite strengthening effect. Dual-Phase steels have been thoroughly studied after the work of Rashid [Rash76, Rash77] who showed that a microstructure consisting of a dispersion of martensite grains in a ferrite matrix can bring about enhanced mechanical properties (figure 1.2). Figure 1.3 suggests how the ferrite-martensite microstructure of Dual-Phase steels is generated by intercritical annealing, i.e. by heating between A_1 and A_3 in the ferrite-austenite phase field, and by subsequently cooling at a rate compatible with austenite transformation to martensite. In the industrial practice, steel compositions were adjusted without a too large increase of costs, in order to obtain the hardenability needed for obtaining martensite with the cooling rate resulting from sheet thickness and quenching capabilities of industrial lines. As a consequence, Dual-Phase steels typically contain low levels of carbon (from 0.05 to 0.15 wt.%), manganese (from 1 to 1.5 wt.%), silicon (around 0.4 wt.%) and sometimes other elements like Cr, Mo or V [Spei81]. During intercritical annealing, the formation of austenite is accompanied by the partitioning of alloying elements between ferrite and austenite [Spei81a, Spei81b, Wycl81, Matl82]. Carbon can concentrate in austenite but the intercritical annealing times are too short (of the order of a few minutes) for allowing redistribution of substitutional alloying elements.

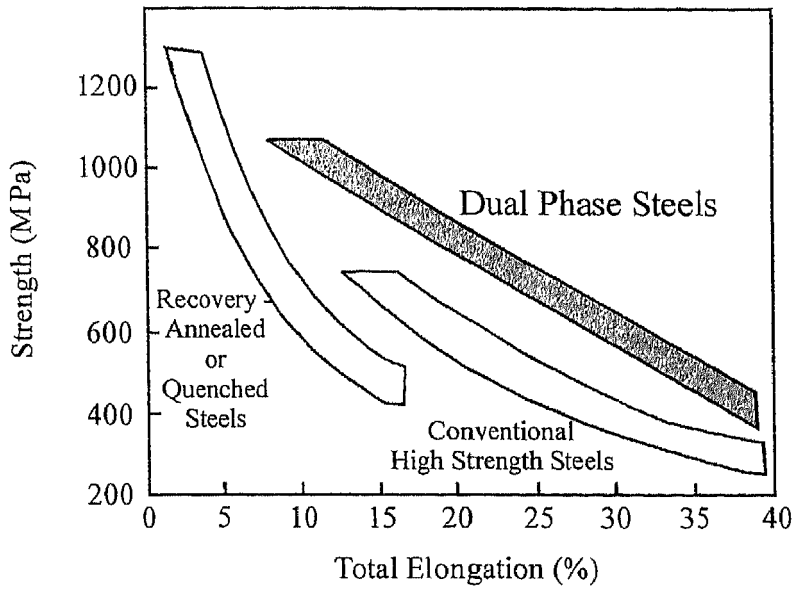

Figure 1.2: Tensile strength as a function of total elongation for 3 types of high-strength steels (from [Matl82]).

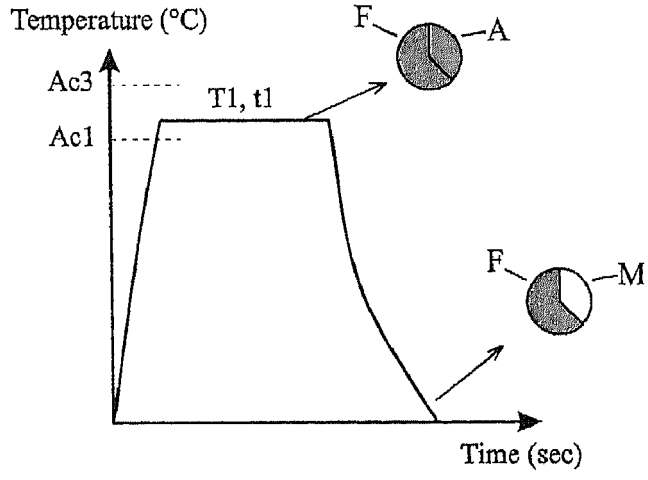

Figure 1.3: Typical heat-treatment scheme of cold-rolled Dual Phase steels.

2.2. Mechanical properties

Numerous studies have been devoted to the relation between *Microstructure and Tensile properties* in Dual-Phase steels [DP77, DP79, DP81, Matl82]. The unique tensile properties of Dual-Phase steels, i.e. low yield strength, high tensile strength and large uniform and total elongations, result from complex interactions of the yielding and strain-hardening behaviours of the microstructural components. The volume fraction, composition, size and distribution of phases can be varied by changes in alloy composition, initial microstructure and processing routes. These microstructural parameters influence in an effective way the mechanical properties. As shown in figure 1.4, the strength of Dual-Phase steels increases with increasing volume fraction of martensite while uniform

elongation (and more globally ductility) decreases. As a consequence, it was generally concluded that better strength-ductility combinations are obtained when martensite constitutes a dispersed phase in the ferrite matrix, i.e. when its volume fraction is around 20-40%.

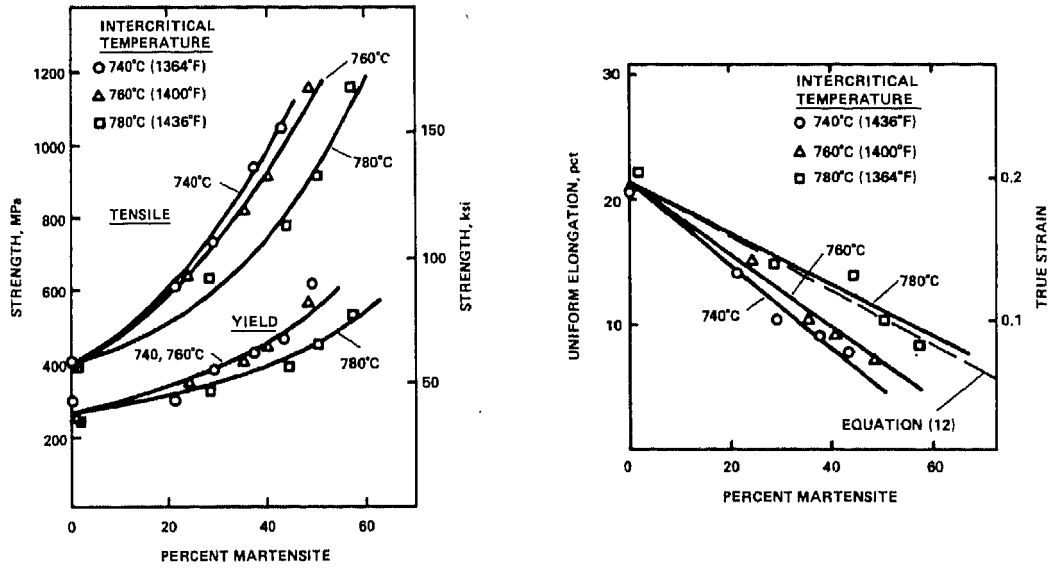

(a) (b)

Figure 1.4: Evolution of yield strength and tensile strength (a) and uniform elongation (b) as a function of the volume fraction of martensite present in microstructure of Dual Phase steels (from [Spei79]).

One of the characteristic features of the mechanical properties of the Dual-Phase steels is the occurrence of continuous yielding instead of the appearance of Lüders bands and the associated 'yield point elongation' generally observed in low alloy steels. This continuous yielding is due to the presence of internal stresses allowing dislocations to remain unpinned by interstitial solutes. These dislocations are generated by the austenite to martensite transformation on cooling. Indeed, martensitic transformation of intercritical austenite in Dual-Phase steels occurs at low temperatures[1] so that the ferrite phase must plastically deform to accommodate the volume expansion (~ 2 to 4 %) and shear deformation ($\gamma \sim 0.24$) arising from the austenite to martensite transformation. As a result, both a high dislocation density and residual stresses are generated in the ferrite phase immediately surrounding martensite particles [Furu79, Rigs79, Spei81a, Rizk82, Bour83]. Furthermore, interactions between the soft ferrite matrix and the hard martensite islands were found in various studies to be the key factors leading to the enhanced mechanical

[1] As all carbon concentrates in austenite during intercritical annealing, this intercritical austenite always presents a low Ms temperature due to the very effective hardening effect associated with carbon [Andr65].

properties of Dual-Phase steels [Rigs79, Rizk82, Bour83, Goel85a, Goel85b]. Martensite transformation on cooling generates free dislocations in the ferrite which contribute to a low yield strength but a high work-hardening rate. In addition, martensite induces an increase of the dislocation density of ferrite and this dislocation strengthening of ferrite determines the high work-hardening rate of Dual-Phase steels.

Finally, several studies have shown that retained austenite with contents up to around 10% can be found beside ferrite and martensite in the microstructure of Dual-Phase steels [Rigs77, Yi83, Sach83]. The question was raised whether this retained austenite can improve the mechanical properties of Dual-Phase steels through the TRIP effect.

3. Mechanically-induced martensitic transformation and the TRIP effect

3.1. Mechanical activation of martensitic transformation

In order to proceed, martensitic transformation, i.e. displacive and diffusionless transformation of parent austenite[2], needs to be accompanied by a decrease in free energy. Figure 1.5 schematically shows the evolution of the chemical free energies of parent austenite and daughter martensite as a function of temperature. For temperatures lower than T_0 (for which the free energies of both phases with identical compositions are identical), the transformation from austenite to martensite is accompanied by a decrease in free energy. However, austenite will not decompose into martensite unless a well-defined 'driving force', i.e. an excess of free energy of austenite over that of martensite, corresponding to the activation barrier is available. As a consequence, martensitic transformation of austenite only occurs at M_s, below a well-defined undercooling ΔT from T_0[3]. As indicated in figure 1.5, a driving force of $\Delta G_{Ms}^{\gamma\alpha'}$ attained for an undercooling

[2] It can be said in a simple way that martensitic transformation arises from a cooperative shear movement of atoms on distances shorter than the atomic inter-distances [Olson92].

[3] The extent of this undercooling and of the corresponding driving force allows an easy distinction between *thermoelastic* and *non-thermoelastic* transformations. As shown in figure 1.6, a substantial difference in transformation hysteresis may be found, indicated by the difference between the A_f and M_s temperatures. The thermoelastic transformation exemplified by the Au-Cd alloy in figure 1.6 or by the well-known Shape Memory Alloys such as Ni-Ti or Cu-Zn-Al [Tamu92], is characterised by a small hysteresis which means a small barrier to transformation and weak dissipative sources. Furthermore, for the thermoelastic case, martensitic transformation proceeds by the continuous growth of martensite plates and the nucleation of new plates on cooling. Direct and reverse transformations either on cooling or heating occur by the forward or backward movements of the martensite/austenite interface. By contrast, for the non-thermoelastic transformation such as for ferrous martensite, once a martensite plate grows to a given size, the interface does not undergo inverse movement during heating.

down to M_s is needed for triggering martensitic transformation. This means that in the absence of any other competing phase transformation[4], austenite cooled at temperatures ranging from M_s to T_0 stays in a metastable state. However, since martensitic transformation is achieved by a cooperative shear movement of atoms, it can be easily envisioned that the mechanical state of the microstructure may influence the transformation. The chemical driving force $\Delta G_{T1}^{\gamma\alpha'}$ at temperature T_1 on figure 1.5, is insufficient for the onset of martensitic transformation. Nevertheless, a mechanical driving force, U, resulting from an externally applied stress may be added to the chemical driving force in order to attain the requested critical driving force $\Delta G_{Ms}^{\gamma\alpha'}$. Consequently, martensitic transformation can be mechanically-induced when a mechanical work supplies the lacking driving force for triggering the transformation [Tamu92, Olson82b, Tamu82].

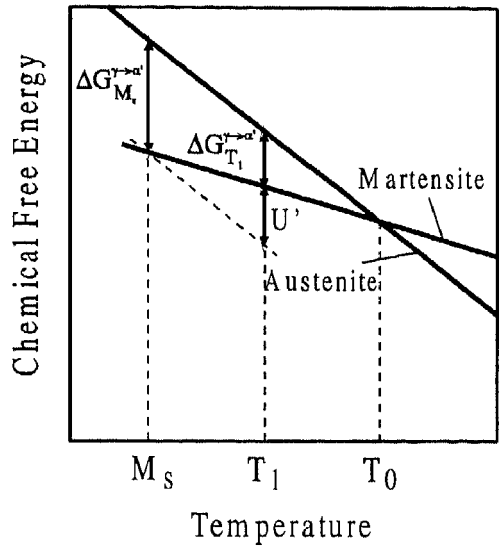

Figure 1.5: Schematic illustration showing chemical free energies of austenite and martensite as a function of temperature.

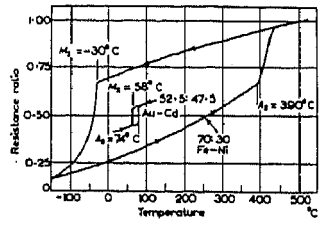

Figure 1.6: Electrical resistance changes during cooling and heating for Fe-Ni and Au-Cd alloys, indicating the hysteresis of the martensite reaction on cooling and the reverse transformation on heating for non-thermoelastic and thermoelastic transformations, respectively (from [Tamu92]).

[4] For steel, the notion of *hardenability* also intervenes in the case of martensitic transformation of austenite since this austenite has to be cooled sufficiently rapidly in order to avoid the other thermally activated phase transformations of parent austenite.

3.2. Stress-assisted and strain-induced martensitic transformation

When austenite is stressed at temperatures above M_s, martensitic transformation thus occurs when a critical stress corresponding to the lacking driving force is attained. Figure 1.7 shows the evolution of this critical applied stress as a function of temperature. As temperature is raised above Ms, the lacking driving force increases and the mechanical work that has to be applied also increases. If the chemical driving force $\Delta G^{\gamma\text{-}\alpha'}$ decreases linearly with temperature above M_s [Patel53], it is expected that the critical applied stress for the onset of martensitic transformation linearly increases when temperature increases. In this regime, the transformation is said to be *stress-assisted* and the mechanical driving force allows martensitic transformation to occur on the same nucleation sites as during cooling. However, when temperature is further raised, the critical stress for triggering transformation reaches the austenite elastic limit (represented by the 0.2% proof stress of austenite in figure 1.7). Austenite will therefore first be plastically deformed before transformation can occur. When austenite is deformed at temperatures above this transition temperature called M_s^{σ} (e.g. at T2 in figure 1.7), austenite which starts to deform plastically at a stress σ_a, has to be strain-hardened up to σ_b before martensitic transformation begins. σ_b is considerably lower than σ_c which could be expected by extrapolating the critical stress versus temperature line valid between M_s and M_s^{σ}. This decrease (σ_c-σ_b) of the critical applied stress for martensite formation is due to the plastic deformation of austenite which creates new potent nucleation sites for martensitic transformation. This regime is called *strain-induced* transformation. The temperature M_s^{σ} corresponds to a reversal of the temperature dependence of the flow stress [Olson78, Haid89a, Tamu92]. It defines the boundary between the temperature regimes where the 2 modes of transformation, i.e. stress-assisted and strain-induced dominate.

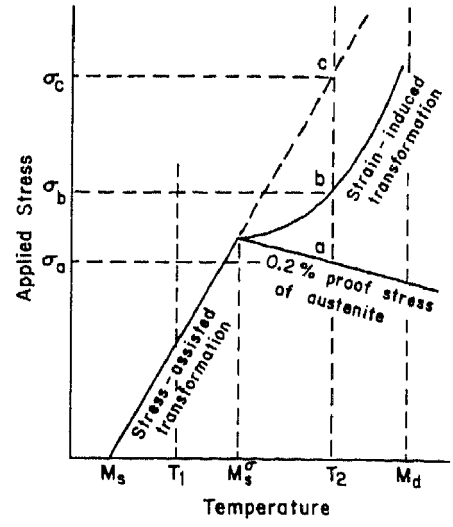

Figure 1.7: Schematic illustration showing the critical stress for martensite formation as a function of temperature.

3.3. Transformation – Induced plasticity, the TRIP effect

Since martensitic transformation can occur during mechanical solicitation, its consequences on the deformation process has been thoroughly studied. It was shown that the aftermath of the mechanically-activated displacive and diffusionless transformation of austenite, such as the dilatational and shear deformations arising from the change of crystal structure, the formation of preferential variants of martensite and the abrupt change of strength [Patel53, Olson75, Onod76, Olson82a, Strin92, Tamu92] improve strength and ductility by shaping the work-hardening rate [Angel54, Zack67, Lud69, Olson78, Olson82b]. These effects of Transformation-Induced Plasticity that are associated with the intrinsic characteristics of the martensitic transformation and with the consequences of the transformation on the surrounding microstructure are classically related to 2 different mechanisms [Lebl89, Mark95, Onod76]: (i) the stress-assisted nucleation of martensitic variants favourably oriented in comparison with the applied stress (Magee mechanism [Magee68]); and (ii) the microscopic plasticity of the phases due to the volume and shape changes associated with the displacive transformation (Greenwood-Johnson effect [Green65]).

Figure 1.8 shows that the balance of mechanical properties such as tensile strength and elongation exhibit an overall optimum when testing is carried out in the temperature range comprised between the M_s temperature of spontaneous martensitic transformation on cooling and the M_d temperature of end of mechanically-induced martensitic

transformation[5]. Tensile strength increases with decreasing test temperature, and this increase almost corresponds to the increase of the martensite content observed in the specimen after fracture. Total elongation exhibits a maximum at the temperature just above M_s^{σ} [6]. This enhancement of elongation is mainly attributed to the suppression of necking due to the increase in work-hardening rate induced by the martensite formation. As a consequence, this TRIP effect was found to be very beneficial for the deformation properties of a wide variety of fully austenitic Fe-Ni-Cr [Angel54, Fahr71, Bhan72], Fe-Ni [Yeo63, Fahr71, Bhan72] or other highly alloyed steels [Tamu92].

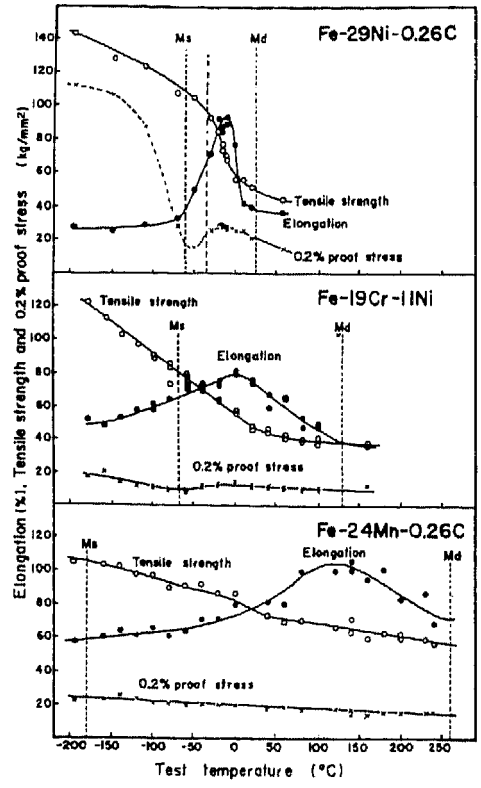

Figure 1.8: Effect of test temperature on tensile properties for three metastable austenitic alloys (from [Tamu92]).

4. Mechanical stability of retained austenite in Dual-Phase steels

Some amount of retained austenite was generally found with ferrite and martensite in Dual-Phase microstructures [Sach83, Goel85a, Yi83, Rigs79]. This austenite was found either as interlath films (or as 'encapsulated') within martensite or as very small isolated

[5] For testing temperatures higher than M_d, the mechanical work needed for the onset of martensitic transformation becomes higher than the level of stress and deformation leading to fracture. In this case, austenite deforms plastically without any transformation until fracture.

[6] Since the balance of mechanical properties influenced by mechanically-induced martensitic transformation show a marked optimum near M_s^{σ}, this temperature has been adopted as a quantitative parameter for characterising of the mechanical stability of retained austenite [Onod76, Tamu92].

grains with a size of the order of a few micrometers [Yi83, Rigs79]. Since Dual-Phase steels do not contain strong austenite stabiliser element[7], other stabilising effects such as a size effect and a matrix constraint effect were asserted to play a role in the retention of austenite in Dual-Phase steels. Furthermore, it was shown that martensitic transformation of this retained austenite can be mechanically-induced during straining so that a TRIP effect occurs in Dual-Phase steels.

While some studies considered this austenite as a minor phase without any effect on the mechanical properties of Dual-Phase steels because of its small volume fraction [Spei79], other works argued that martensitic transformation of retained austenite during deformation improves mechanical properties of Dual-Phase steels by increasing the work-hardening rate thanks to the generation of a greater dislocation density in ferrite [Rigs77]. However, this retained austenite transforms very rapidly in the early stage of straining in such a way that after only a few percents of plastic strain, austenite content is completely exhausted and the TRIP effect cannot anymore affect the work-hardening rate. It was therefore suggested that the mechanical stability of retained austenite is the key factor susceptible of inducing a more effective enhancement of the mechanical properties of Dual-Phase steels thanks to the TRIP effect.

In the fully austenitic TRIP steels (as well as in other iron-based alloys containing retained austenite as a dispersed phase capable of mechanically-activated martensitic transformation), the mechanical stability of austenite was generally tuned in order to induce the martensitic transformation in the optimal way at the considered test temperature. As shown in figure 1.8, optimum mechanical properties of the fully austenitic TRIP steels are obtained at a well defined temperature near M_s^{σ} which depends on the chemical composition (that determines M_s) and on the applied stress state (that determines the effectiveness of the mechanical activation of the transformation). Several studies [Zack67, Angel54, Bhan72, Fahr71] have shown how the chemical composition of these fully austenitic TRIP steels can be adjusted in order to improve their mechanical properties at room temperature. Particular heat-treatment schemes were also necessary for adapting the mechanical stability of retained austenite dispersed in other iron-based alloys such as Maraging steels [Katz83], high Ni-Co secondary hardening martensitic steels [Haid87, Haid88], Fe-Ni alloys [Yano73, Fultz85] and Ultra High-Strength steels [Haid88, Haid89b] so that retained austenite could effectively enhance strength, ductility or toughness.

[7] except carbon that concentrates within intercritical austenite. However, the global carbon contents involved in typical chemical compositions and the volume fractions of intercritical austenite allow only marginally a lowering of M_s under the quenching temperature.

Although the mechanical stability of retained austenite in Dual-Phase steels is quite rigidly fixed by the chemical composition and the imposed heat-treatment, Sachdev [Sach83] and Goel et.al. [Goel85a, Goel85b] have experimentally or theoretically shown that a greater mechanical stability of austenite should lead to improved mechanical properties.

As in the case of fully austenitic TRIP steels, Sachdev [Sach83] has considered the mechanical stability of retained austenite of Dual-Phase steels and its effect on mechanical properties by investigating the effect of testing temperature. As shown in figure 1.7, an increase of the testing temperature is accompanied by an increase of the mechanical driving force needed for triggering martensitic transformation. Figure 1.9 shows that, indeed, retained austenite transforms less rapidly during plastic straining when the testing temperature is increased above room temperature. As a consequence, Sachdev [Sach83] showed that the ductility of the investigated Dual-Phase steel is increased by nearly 50% compared to room temperature with no loss of strength when tensile testing is carried out around 80°C.

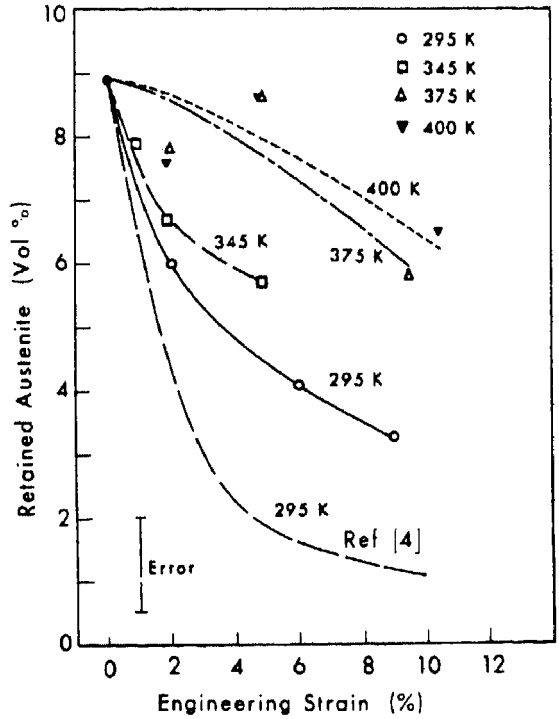

Figure 1.9: Volume fraction of retained austenite as a function of engineering strain for different testing temperatures of a 0.12C – 1.4Mn – 0.5Si – 0.06 V Dual Phase steels (from [Sach83]).

On the other hand, Goel et. al. [Goel85a, Goel85b] have developed a theoretical model describing the flow behaviour of Dual-Phase steels that takes into account of the mechanically-induced martensitic transformation of retained austenite. The parameters

describing the mechanical stability of austenite were allowed to be change. Figure 1.10 presents stress-strain curves generated by this model for a microstructure consisting of 70% of ferrite, 20% of martensite and 10% of austenite with various stabilities. While retained austenite of Dual-Phase steels can be considered as *'highly unstable'* so that martensitic transformation shows weak influence on the overall mechanical properties, figure 1.10 shows that *'moderately stable'* austenite brings about an effective improvement of the strength-ductility balance by inducing a higher work-hardening rate during the major part of plastic strain.

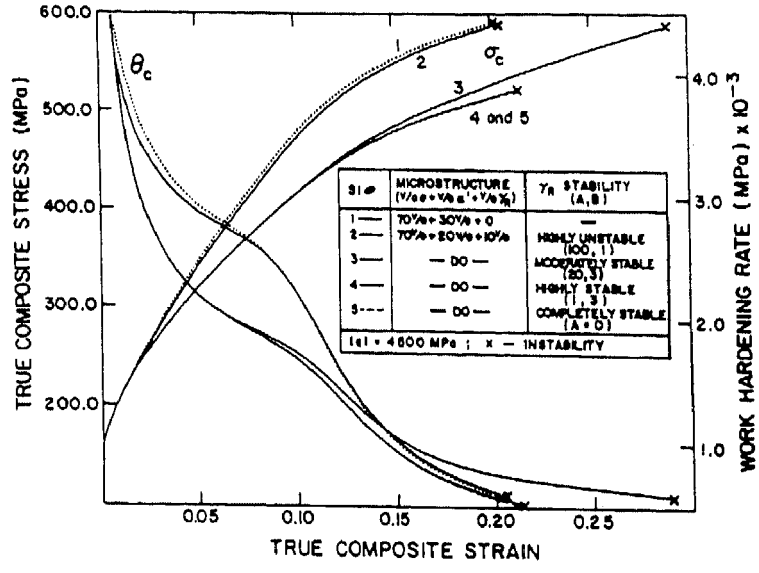

Figure 1.10: Calculated true composite stress and work-hardening rate as a function of true composite strain for a Dual Phase steel containing 70%, 20% and 10% of ferrite, martensite and retained austenite with varying stability, respectively (from [Goel85b]).

Considering these 2 results, it can be concluded that the unique strength – ductility combinations of Dual-Phase steels could be further enhanced if retained austenite (quite inevitably present in their microstructures) would exhibit a higher mechanical stability in such a way that its transformation all along plastic deformation could increase the work-hardening rate. However, this increase of stability should not be obtained at the expense of increasing costs by the addition of costly austenite stabiliser alloying elements such as Ni[8].

Nevertheless, Dual-Phase steels contain sufficient contents of carbon (which is a very strong austenite stabiliser element) for bringing about an adequate mechanical stability of

[8] Dual-Phase steels as well as the so-called 'High-Strength Low Alloy' steels are foreseen for large scale industrial applications. Production costs therefore intervene as a strong constraint in the development of these steel grades. This is the case with the HSLA steels for which enhanced mechanical properties were achieved through only micro-additions of alloying elements and controlled hot-rolling.

substantial amounts of austenite at room temperature if this further carbon enrichment of this austenite can be achieved following the first enrichment occurring during intercritical annealing. Such a further enrichment can result from the intrinsic characteristics of *bainite transformation* (which is certainly the most complex mechanism of phase change in steels).

5. Austenite retention through bainite transformation

5.1. High-Strength, High-Toughness bainitic steels

The well-known 'quenched and tempered' martensitic steels are high-strength steels also exhibiting high toughness properties. In this case, precipitation of fine carbides is controlled during tempering of supersaturated martensite. Even though bainitic microstructures present relatively high strength, these microstructures are not widely used in technological applications because of the presence of coarse carbides reducing ductility and toughness. In plain carbon steels, bainitic microstructures consist of packets of lath-shaped ferrite separated by coarse cementite particles. It has been observed [Bhad90, Ohmo91, Taka91, Bhad92b], that silicon strongly retards the precipitation of cementite during the bainite reaction, therefore bringing about a microstructure consisting of laths of ferrite and carbon rich austenite. This combination of high-strength bainitic ferrite and ductile austenite was reported to drastically enhance strength and toughness properties of bainitic steels [Sand81, Bhad83a, Bhad83b, Miihk87a, Miihk87b, Miihk87c, Edmon90, Tomi93] when heat-treatment was conducted in such a way that mechanical stability of austenite was well adjusted. Large contents of retained austenite can thus be found in the microstructure of steels with rather simple compositions containing a sufficient amount of silicon. The presence of this retained austenite is not fortuitous but results from the intrinsic mechanisms of the bainite transformation.

5.2. The bainite transformation

5.2.1. Main features of bainite

Bainite transformation occurs in a temperature range situated between the range where pearlite is formed from the cooperative growth of ferrite and cementite is formed, and the temperature range below M_s where austenite transforms into martensite. Bainite can be considered as a non-lamellar aggregate of ferrite and carbides with a particular morphology described as acicular or 'in sheaves' [Taka91]. Bainite thus forms by different mechanisms

than pearlite. Indeed, during the decomposition of austenite to pearlite, ferrite and cementite crystals grow cooperatively at a common transformation front with the parent austenite. Their growth rates are coupled, and their compositions are complementary in the sense that the excess solute displaced by the growth of ferrite is incorporated into cementite. The situation is totally different for bainite. It is well established now [Bhad92a] that bainite transformation can be divided in 2 separable stages: a stage of growth of ferrite followed eventually by a stage of precipitation of carbides. As a matter of fact, the mechanisms intervening in the bainite transformation have remained quite controversial up to today. Even if it was clear from the very beginning research on bainite that bainite transformation exhibits many of the features commonly observed in the martensitic transformation in steels[9], most of the early works felt uneasy about the fact that bainite reaction proceeded at a comfortably observable rate, whereas the martensite growth rate was known to be limited only by the speed of sound in the metal [Bhad92b, Bhad92c]. Bainite formation thus associates features commonly attributed to martensitic transformation and features more similar to pearlite decomposition such as carbon diffusion and redistribution.

Bainite was shown to consist of aggregates of thin lenticular platelets or laths of ferrite separated by regions of *residual* phases consisting of untransformed austenite or of martensite or cementite having formed subsequently to the growth of bainitic ferrite. The aggregates of bainitic platelets are generally called *'sheaves'*. Furthermore, the platelets tend to adopt almost the same crystallographic orientation within a given sheaf. The growth of each sub-unit is accompanied by a shape change with a large shear component. This shape strain causes plastic deformation of austenite that seems responsible for the fact that each sub-unit grows to a limited size which may be lower than the austenite grain size. Consequently, the sheaf as a whole grows by the repeated appearance of new sub-units which nucleate mostly near the tips of the already existing sub-units.

A common distinction is made between *upper bainite* and *lower bainite* depending on the place where carbide precipitation occurs. Bainite transformation is indeed accompanied by carbon redistribution following the formation of bainitic ferrite. At relatively high temperatures, upper bainite is formed, which consists of sheaves of ferrite platelets with cementite particles trapped between the platelets. As a consequence of the transformation mechanism, the austenite that is trapped between platelets becomes enriched in carbon so

[9] As an intermediate phase between pearlite and martensite, it was envisioned that bainite could be related to one of the mechanisms intervening in each phase change, (i) reconstructive phase transformation for pearlite, involving a complete reconstruction of the new crystallographic lattice by uncoordinated migration of atoms; or (ii) displacive formation of martensite without any diffusion but only a lattice change by coordinated movements of the iron and substitutional atoms [Hehe70].

that cementite precipitation occurs adjacently to the ferrite platelets. At a lower temperature, lower bainite is formed, which also consists of a non-lamellar aggregate of ferrite and carbides. Lower bainite, however, contains 2 kinds of carbides. Like for upper bainite, some carbides precipitate from the enriched austenite between the bainitic ferrite platelets. In addition, lower bainite usually contains a fine dispersion of carbides within the lenticular ferrite plates.

5.2.2. Mechanism of bainite formation

Bainite transformation can be considered as a slow, diffusionless transformation involving a number of successive or competitive events.

Figure 1.11 represents schematically how a sheaf of upper bainite propagates through an austenite grain. A lenticular platelet of ferrite first nucleates at an austenite grain boundary and lengthens towards the grain interior until its growth is stifled by the plastic deformation of surrounding austenite. A second plate then nucleates at the tip of the first and a sheaf of bainite propagates through the austenite grain by this process of successive nucleation and growth of individual sub-units. As suggested in figure 1.11, the growth rate of platelets is much faster than the growth rate of the sheaf as a consequence of these repeated nucleation events intervening as the rate-controlling process. This formation of bainitic ferrite platelets occurs by a displacive phase transformation process without redistribution of substitutional or interstitial alloying elements. However, the temperature at which bainite transformation occurs allows the excess carbon to be rejected from ferrite into surrounding not yet transformed residual austenite. As illustrated in figure 1.11, the carbon content of bainitic ferrite decreases while residual austenite from which the next ferrite platelets have to grow shows an increase of carbon content until the beginning of cementite precipitation. The sheaf morphology of upper bainite thus results from the reactions of decomposition of austenite into either ferrite and/or cementite.

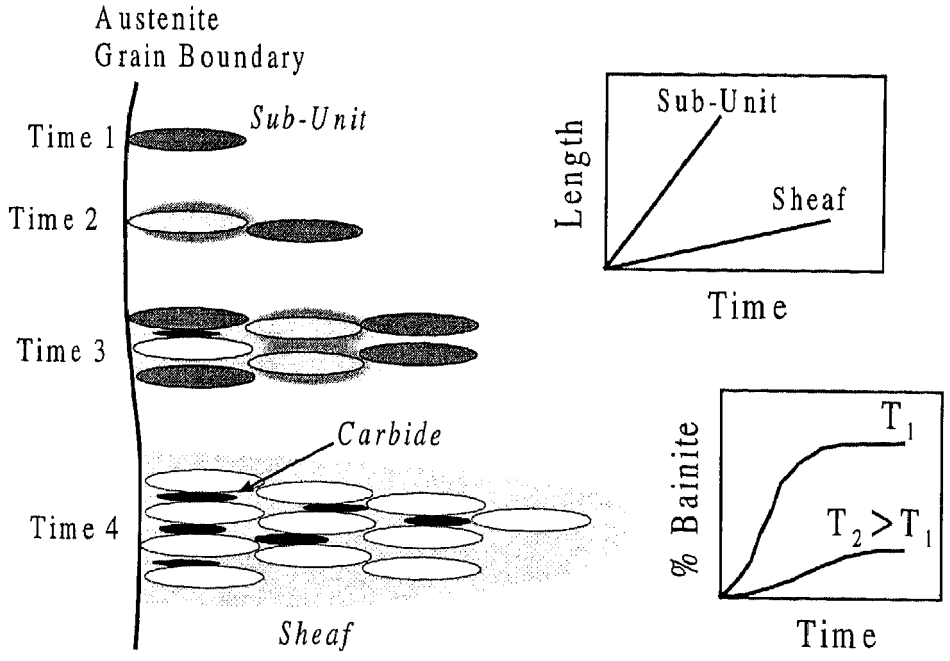

Figure 1.11: Schematic representation of the development of a sheaf of bainite as well as illustration of microstructural and kinetic features of the bainite transformation (following [Bhad92a]).

In view of this process of formation of bainite, the distinction between upper bainite and lower bainite can be easily understood by comparing the time required to decarburise bainitic ferrite platelets with the time required to precipitate cementite. Figure 1.12 schematically represents both cases. If carbon redistribution is fast because it occurs at high temperatures, i.e. if the decarburisation process dominates, no cementite can precipitate within ferrite platelets in such a way that upper bainite is formed. On the contrary, in cases of a relatively rapid carbide precipitation within ferrite or of a high carbon supersaturation, all carbon cannot be easily rejected from ferrite, which leads to the formation of lower bainite.

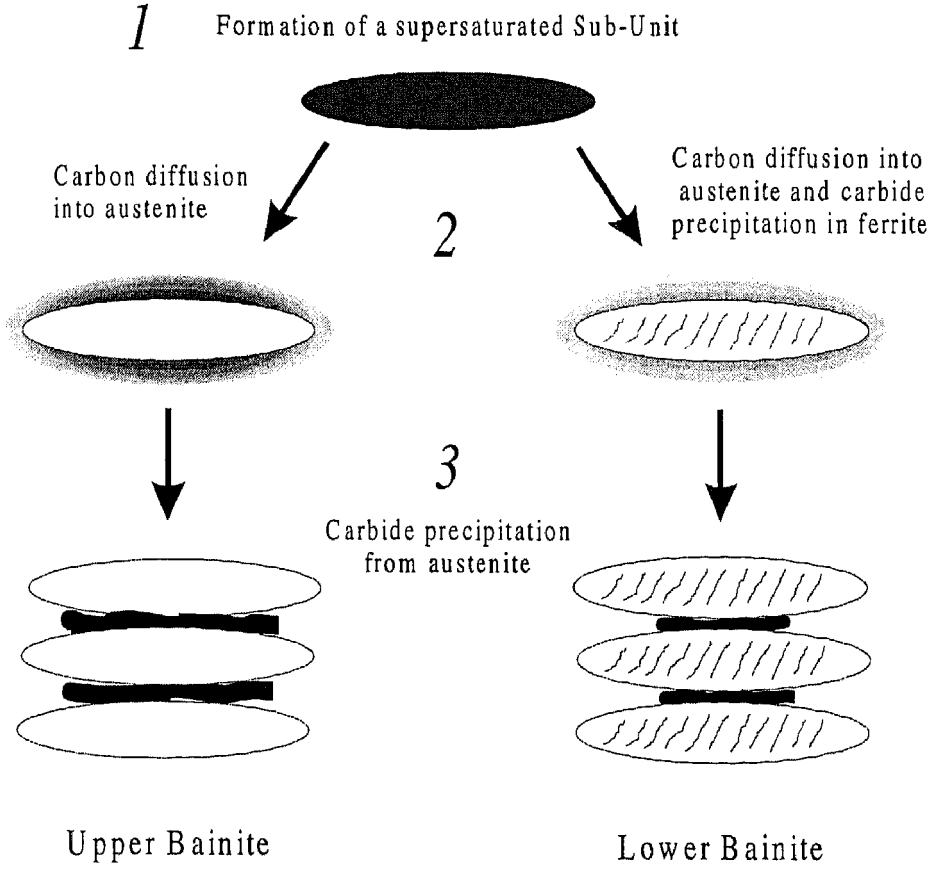

Figure 1.12: Schematic illustration of the formation of either upper bainite or lower bainite (following [Bhad92a]).

5.2.3. Bainite transformation and retention of austenite

The main feature of bainite transformation *helpful* for the retention of austenite is the redistribution of carbon accompanying the progress of the transformation. From this point of view, cementite precipitation during the formation of bainitic ferrite is not essential to the progress of the transformation as it can be considered as a secondary process occurring after the main step of the transformation, that is the displacive formation of bainitic ferrite. Actually, carbide-free bainite consisting of a mixture of bainitic ferrite and austenite is found in some alloys in which carbide precipitation is totally inhibited or sufficiently slowed so that it does not accompany the formation of bainitic ferrite. Cementite precipitation is effectively inhibited in iron-based alloys containing substantial amounts of silicon (or sometimes aluminium). The effect of silicon is generally attributed to the fact that silicon solubility in cementite is very small. It is therefore proposed that, in high silicon steels, silicon poor regions have to be formed within austenite for allowing the precipitation of cementite and that the need for substitutional silicon to diffuse away from

the cementite/ferrite interface at relatively low temperatures could explain the retardation of the cementite growth.

Carbon enrichment of residual austenite accompanies therefore the progress of the bainite transformation in high silicon steels in such a way that this austenite can be retained at room temperature. However, this process stops before the complete consumption of austenite and at an austenite volume fraction that depends on the bainite transformation temperature. Indeed, although cementite precipitation is not essential to the occurrence and progress of the bainite transformation, the hindering of cementite precipitation leads to the locking of the transformation before it is completed. This phenomenon is known as the *incomplete reaction phenomenon* and finds its origin in the mechanism of diffusionless phase transformation of austenite to bainitic ferrite. Figure 1.13 presents schematic free energies curves of ferrite and austenite as a function of carbon content at temperature T_1 as well as the corresponding phase diagram. The common tangent to the free energies curves allows finding on the phase diagram the carbon concentrations of the equilibrium boundaries Ae_1 and Ae_3. The formation of bainitic ferrite by the displacive phase transformation of austenite does not involve diffusion. Figure 1.13 shows that only austenite with a carbon content lower than x_{T0} (where ferrite and austenite of identical composition have identical free energy) can transform into ferrite of identical composition with a reduction of free energy. This thermodynamic condition for diffusionless transformation of austenite to ferrite therefore fixes the upper bound for the carbon content of austenite, which is represented on the phase diagram of figure 1.13 by the curve T_0. This means that, in the absence of cementite precipitation reducing the carbon content of austenite, bainitic ferrite platelets nucleate and grow from increasingly carbon enriched austenite (and further increase this enrichment by rejecting excess carbon) until carbon content of residual austenite reaches the value dictated by the thermodynamical condition for diffusionless growth. When this carbon content given by the T_0 curve is reached, the transformation stops, leaving the residual austenite untransformed. Further holding at the same temperature does not lead to any progress of bainite transformation[10]. As illustrated in figure 1.11, due to the negative slope of the T_0 curve, bainite transformation stops at a more early stage when the holding temperature is higher.

[10] This stasis in the transformation of austenite by a displacive and diffusionless transformation does not mean that other mechanisms of austenite transformation such as a reconstructive transformation into ferrite cannot occur. However, due to the relatively low temperatures where bainite transformation takes place, this process is very slow. Furthermore, further progress of the bainite transformation of austenite can occur if carbon content of residual austenite is reduced by cementite precipitation.

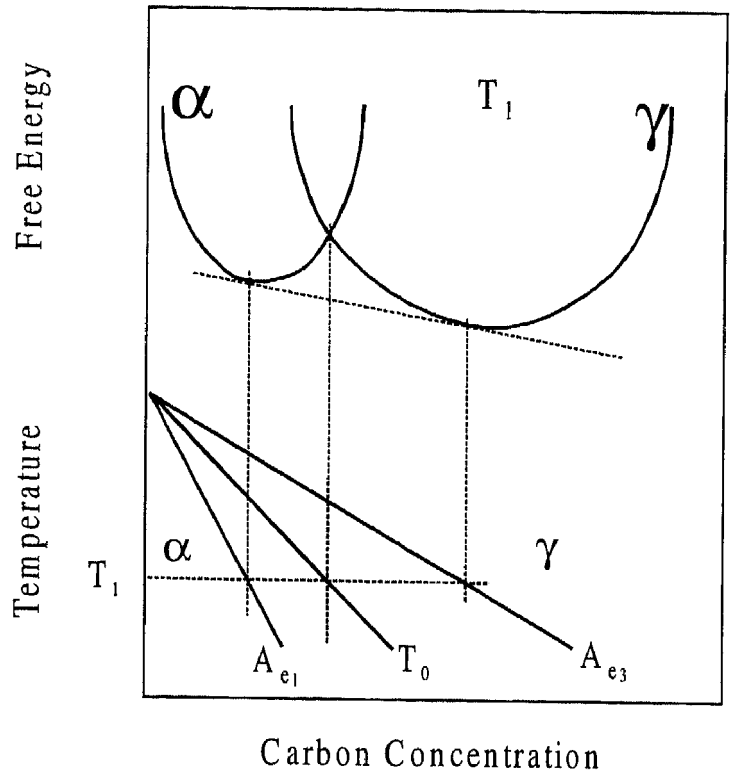

Figure 1.13: Schematic illustration of the origin of the T_0 curve on a phase diagram as resulting at each temperature of specific points of the free energy curves of ferrite and austenite (from [Bhad92c]).

In conclusion, the carbon redistribution during bainite transformation and the inhibition of cementite precipitation from residual austenite by silicon allow effective enrichment of austenite by carbon which is known to be the most potent austenite stabiliser. This process is used in high performance bainitic steels in which retained austenite was shown to have a beneficial influence on the mechanical properties.

6. Emergence of the TRIP-assisted multiphase steels

The characteristics of the TRIP-assisted multiphase steels results from the synthesis of the positive effect of each phenomenon presented above.

Like Dual-Phase steels, TRIP-assisted multiphase steels also present a microstructure consisting of more than one phase as a result of the intercritical annealing dwell. As shown in figure 1.14, whereas Dual-Phase steels are directly quenched to room temperature after intercritical annealing, TRIP-aided steels are quenched to an intermediate temperature

range of 350 – 450°C for an isothermal bainitic tempering[11]. As for high performance bainitic steels, this tempering allows further carbon enrichment of residual austenite so that the stability of austenite at room temperature is effectively enhanced in comparison with that retained austenite in Dual-Phase steels. In order to allow this carbon enrichment, TRIP-assisted multiphase steels commonly contain large concentrations of silicon (from 1.5 to 2.5 wt.%) in order to inhibit cementite precipitation during bainitic tempering. These levels of silicon are of the same order as in the high performance bainitic steels, i.e. about 1.5 wt.% larger than in typical Dual-Phase steels [Spei81a]. Furthermore, as Dual-Phase steels, TRIP-aided steels also contain from 0.1 to 0.4 wt.% of carbon and from 1.5 to 2.5 wt.% of manganese. With these chemical compositions and the 2 stage heat-treatment described in figure 1.14, contents of austenite of the order of 5-20% [Saku91, Akis95] can be retained in the microstructure. Beside this austenite, TRIP-assisted multiphase steels also contain idiomorphic ferrite, bainite and sometimes martensite. Like in the fully austenitic TRIP steels, this retained austenite transforms during straining, giving rise to the TRIP effect.

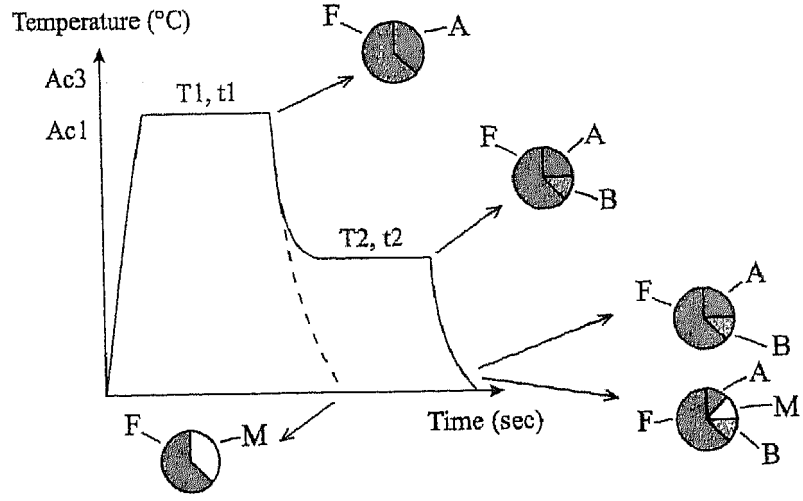

Figure 1.14: Typical heat-treatment scheme of cold-rolled TRIP-assisted multiphase steels.

However, even if it seems evident at this point that a historical or causal relationship can be established between the TRIP-assisted multiphase steels and the various iron-based alloys described above, these connections have been hardly explicitly revealed in the literature. Nevertheless, this work will try in the next chapters to further enlighten the correlation existing with other iron-based alloys as well as the unique features that make the TRIP-assisted multiphase steels a completely new material.

[11] In the following chapters, *'bainitic tempering'* will refer to this isothermal holding in the bainite transformation temperature range prior to quenching to room temperature.

7. Conclusion

This chapter has tried to give a first insight into the characteristics of the TRIP-assisted multiphase steels by replacing them into the general context of the various iron-based alloys to which they can be related. Some relevant results concerning Dual-Phase steels have been exposed. The TRIP effect was briefly described as a supplementary strengthening mechanism. Owing to the poor mechanical stability of the retained austenite found in Dual-Phase steels, it was shown how the intrinsic features of the bainite transformation can bring about stabilisation of austenite through a redistribution of carbon. This chapter constitutes only a first insight into the unique features and properties of TRIP-assisted multiphase steels. The next chapters will focus more precisely on each aspect of these steels, and will also show how a newly developed low silicon steel can partly respond to the various needs evoked in this chapter.

References

[Akis95] O. Akisue, and T. Hada: *Nippon Steel Tech. Rep.*, 1995, vol. 64, pp. 1-6

[Andr65] K.W. Andrews: *J. Iron and Steel Inst.*, 1965, pp. 721-727

[Angel54] T. Angel: *J. Iron and Steel Inst.*, 1954, pp. 165-174

[Bhad83a] H.K.D.H. Bhadeshia, and D.V. Edmonds: *Metal Science*, 1983, vol. 17, pp. 411-419

[Bhad83b] H.K.D.H. Bhadeshia, and D.V. Edmonds: *Metal Science*, 1983, vol. 17, pp. 420-425

[Bhad90] H.K.D.H. Bhadeshia, and J.W. Christian: *Metall. Trans. A*, 1990, vol. 21A, pp. 767-797

[Bhad92a] H.K.D.H. Bhadeshia: *Bainite in Steels*, The Institute of Materials, London, 1992

[Bhad92b] H.K.D.H. Bhadeshia: *Bainite in Steels*, The Institute of Materials, London, 1992, pp. 124-194

[Bhad92c] H.K.D.H. Bhadeshia: *Bainite in Steels*, The Institute of Materials, London, 1992, pp. 1-19

[Bhan72] D. Bhandarkar, V.F. Zackay, and E.R. Parker: *Metall. Trans.*, 1972, vol. 3, pp. 2619-2631

[Bour83] D.L. Bourell, and A. Rizk: *Acta Metall.*, 1983, vol. 31(4), pp. 609-617

[Davi79] R.G. Davies, C.L. Magee: *Proc. Conf. Structure and Properties of Dual-Phase Steels*, R.A. Kot and J.W. Morris ed., TMS-AIME, 1979, pp. 1-19

[DP77] *Formable HSLA and Dual-Phase Steels*, A.T. Davenport ed., TMS-AIME, 1977

[DP79] *Proc. Conf. Structure and Properties of Dual-Phase Steels*, R.A. Kot and J.W. Morris ed., TMS-AIME, 1979

[DP81] *Fundamentals of Dual-Phase Steels*, R.A. Kot and B.L. Bramfitt ed., TMS-AIME, 1981

[Edmon90] D.V. Edmonds, and R.C. Cochrane: *Metall. Trans. A*, 1990, vol. 21A, pp. 1527-1540

[Fahr71] D. Fahr: *Metall. Trans.*, 1971, vol. 2, pp. 1883-1892

[Fultz85] B. Fultz, J.I. Kim, Y.H. Kim, H.J. Kim, G.O. Fior, and J.W. Morris: *Metall. Trans. A*, 1985, vol. 16A, pp. 2237-2249

[Furu79] T. Furukawa, H. Morikawa, H. Takechi, and K. Koyama: *Proc. Conf. Structure and Properties of Dual Phase Steels*, R.A. Kot and J.W. Morris ed., TMS-AIME, Warrendale, PA, 1979, pp. 281-303

[Goel85a] N.C. Goel, S. Sangal, K. Tangri: *Metall. Trans. A*, 1985, vol. 16A, pp. 2013-2021

[Goel85b] S. Sangal, N.C. Goel, K. Tangri: *Metall. Trans. A*, 1985, vol. 16A, pp. 2023-2029

[Green65] G.W. Greenwood, and R.H. Johnson: *Proc. Roy. Soc. London, Ser. A*, 1965, vol. 283, pp. 403-422

[Haid87] G.N. Haidemenopoulos, G.B. Olson, and M. Cohen: *Proc. 34th Sagamore Army Materials Research Conf.*, Lake George, New York, 1987, pp. 549-593

[Haid88] G.N. Haidemenopoulos: PhD thesis, MIT, 1988

[Haid89a] G.N. Haidemenopoulos, M. Grujicic, G.B. Olson, and M. Cohen: *Acta Metall.*, 1989, vol. 37(6), pp. 1677-1682

[Haid89b] G.N. Haidemenopoulos, G.B. Olson, M. Cohen, K. Tsuzaki: *Scripta Metall. Mater.*, 1989, vol. 23, pp. 207-212

[Hehe70] R.F. Hehemann: *Phase Transformations*, ASM, Metals Park, Ohio, 1970, pp. 397-432

[Katz83] Y. Katz, H. Mathias, S. Nadiv: *Metall. Trans. A*, 1983, vol. 14A, pp. 801-808

[Lebl89] J.B. Leblond, J. Devaux, and J.C. Devaux: *Int. J. Plasticity*, 1989, vol. 5, pp. 551-572

[Lud69] D.C. Ludwigson, and J.A. Berger: *J. Iron and Steel Inst.*, 1969, pp. 63-69

[Magee68] C.L. Magee, and H.W. Paxton: *Trans. Metall. Soc. AIME*, 1968, vol. 242, pp. 1741-1749

[Mark95] F. Marketz, and F.D. Fischer: *Metall. Trans. A*, 1995, vol. 26A, pp. 267-278

[Matl82] D.K. Matlock, F. Zia-Ebrahimi, G. Krauss: *Deformation, processing and structures*, G. Krauss, ed. ASM, 1982, pp. 47-87

[Miihk87a] V.T.T. Miihkinen, and D.V. Edmonds: *Mater. Sc. Technol.*, 1987, vol. 3, pp. 422-431

[Miihk87b] V.T.T. Miihkinen, and D.V. Edmonds: *Mater. Sc. Technol.*, 1987, vol. 3, pp. 432-440

[Miihk87c] V.T.T. Miihkinen, and D.V. Edmonds: *Mater. Sc. Technol.*, 1987, vol. 3, pp. 441-449

[Ohmo91] Y. Ohmori, and T. Maki: *Mater. Trans. JIM*, 1991, vol. 32, pp. 631-641

[Olson75] G.B. Olson, and M. Cohen: *Metall. Trans. A*, 1975, vol. 6A, pp. 791-795

[Olson78] G.B. Olson, and M. Azrin: *Metall. Trans. A*, 1978, vol. 9A, pp. 713-721

[Olson82a] G.B. Olson, and M. Cohen: *Metall. Trans. A*, 1982, vol. 13A, pp. 1907-1914

[Olson82b] G.B. Olson: *Deformation, processing and structures*, G. Krauss, ed. ASM, 1982, pp.391-424

[Olson92] G.B. Olson: *Martensite*, G.B. Olson and W.S. Owen ed, ASM, 1992, pp. 1-10

[Onod76] H. Onodera, H. Goto, and I. Tamura: *Proc. 1st JIM Int. Symp. New Aspects of Martensitic Transformations*, Kobe, Japan, 1976, pp. 327-338

[Patel53] J.R. Patel, and M. Cohen: *Acta Metall.*, 1953, vol. 1, pp. 531-538

[Rash76] M.S. Rashid: *SAE Preprint 760202*, 1976

[Rash77] M.S. Rashid: *SAE Preprint 770211*, 1977

[Rigs77] J.M. Rigsbee, P.J. VanderArend: *Formable HSLA and Dual-Phase Steels*, A.T. Davenport ed., TMS-AIME, 1977, pp.56-86

[Rigs79] J.M. Rigsbee, J.K. Abraham, A.T. Davenport, J.E. Franklin, and J.W. Pickens: *Proc. Conf. Structure and Properties of Dual Phase Steels*, R.A. Kot and J.W. Morris ed., TMS-AIME, Warrendale, PA, 1979, pp. 304-329

[Rizk82] A. Rizk, and D.L. Bourell: *Scripta Metall.*, 1982, vol. 16, pp. 1321-1324

[Sach83] A.K. Sachdev, *Acta Metall.*, 1983, vol. 31(12), pp. 2037-2042

[Saku91] Y. Sakuma, O. Matsumura, and O. Akisue: *ISIJ Int.*, 1991, vol. 31, pp. 1348-1353

[Sand81] B.P.J. Sandvik, and H.P. Nevalainen: *Metals Technol.*, 1981, pp. 213-220

[Spei79] G.R. Speich, R.L. Miller: *Proc. Conf. Structure and Properties of Dual Phase Steels*, R.A. Kot and J.W. Morris ed., TMS-AIME, Warrendale, PA, 1979, pp. 145-182

[Spei81a] G.R. Speich: *Fundamentals of Dual-Phase Steels*, R.A. Kot and B.L. Bramfitt ed., TMS-AIME, 1981, pp. 3-45

[Spei81b] G.R. Speich, V.A. Demarest, R.L. Miler: *Metall. Trans. A*, 1981, vol. 12A, pp. 1419-1428

[Strin92] R.G. Stringfellow, D.M. Parks, and G.B. Olson: *Acta Metall. Mater.*, 1992, vol. 40(7), pp. 1703-1716

[Taka91] M. Takahashi, and H.K.D.H. Bhadeshia: *Mater. Trans. JIM*, 1991, vol. 32, pp. 689-696

[Tamu82] I. Tamura: *Metal Sc.*, 1982, vol. 16, pp. 245-253

[Tamu92] I. Tamura, and C.M. Wayman: *Martensite*, G.B. Olson and W.S. Owen ed, ASM, 1992, pp. 227-242

[Tomi93] Y. Tomita, and T. Okawa: *Mater. Sc. Eng. A*, 1993, vol. 172A, pp. 145-151

[Wycl81] P. Wycliffe, G.R. Purdy, J.D. Embury: *Fundamentals of Dual-Phase Steels*, R.A. Kot and B.L. Bramfitt ed., TMS-AIME, 1981, pp. 59-84

[Yano73] S. Yano, H. Sakurai, H. Mimura, N. Wakita, T. Ozawa, and K. Aoki: *Trans. ISIJ*, 1973, vol. 13, pp. 133-140

[Yeo63] R.B.G. Yeo: *Trans. Metall. Soc. AIME*, 1963, vol. 227, pp. 884-890

[Yi83] J.J. Yi, K.J. Yu, I.S. Kim, S.J. Kim: *Metall. Trans. A*, 1983, vol. 14A, pp. 1497-1504

[Zack67] V.F. Zackay, E.R. Parker, D. Fahr, and R. Busch: *Trans. Am. Soc. Met.*, 1967, vol. 60, pp. 252-259

Chapter II

Materials and Experimental Procedures

This chapter describes the different steels investigated in this thesis as well as the experimental procedures designed and used in order to enlighten the factors governing the properties of TRIP-assisted multiphase steels. The chemical compositions and the 'pre-processing' conditions of the studied steels will first be described. We will then show how thermal processes were conducted as well as present the techniques used for the investigation of the mechanical properties. This chapter will finally summarise the particular procedures developed for the metallographic characterisation of the complex microstructure of TRIP-assisted multiphase steels and, particularly of the retained austenite. However, for the sake of clarity, the specific materials and experimental procedures used in the different parts of this thesis will be reminded at the beginning of each chapter.

1. Materials

1.1 Chemical compositions

Three steels called *HSiI*, *HSiII* and *LSi* are investigated in this thesis. Their respective chemical compositions together with the Ac_1 and Ac_3 transformation temperatures measured by dilatometry are given in Table 2.1. Steels HSiI and HSiII correspond to usual compositions of TRIP-assisted multiphase steels with a rather high silicon content (~ 1.5wt.%), some manganese (~ 1.4wt.%) and 2 different levels of carbon, 0.13 and 0.29wt.% respectively. Steel LSi presents a much lower silicon content (0.38wt.%) while its manganese and carbon contents are similar as in steel HSiI. With this chemical composition, steel LSi is comparable to typical cold-rolled Dual-Phase steels [Spei81a]. The different investigations carried out in this thesis will in each case compare one of the conventional TRIP-aided steels (HSiI or HSiII) with steel LSi. Steel LSi will reveal to constitute a new type of very effective high-strength formable steel.

(10^{-3} wt.%)	C	Mn	Si	P	S	Cr	Ni	Cu	Nb	Al	N	Ac_1	Ac_3
HSiI	130	1420	1500	13	9	13	20	8	0	27	7.9	745	860
HSiII	290	1420	1410	12	20	3	7	4	0	40	8	740	850
LSi	160	1300	380	13	12	19	27	19	13	30	6.3	721	840

Table 2.1: Chemical compositions (10^{-3} wt.%) of the investigated steels.

1.2 Hot-rolling and cold deformation

Steel LSi is an industrially produced alloy. Hot-rolled plates of this steel with 5.5mm thickness were supplied by Cockerill-Sambre[1]. Hot-rolling was conducted following classical practice. Figure 2.1 presents light micrographs of the as hot-rolled microstructure of steel LSi. Figure 2.1(a) shows that hot-rolling resulted in a fine-grained microstructure constituted by ferrite and pearlite. On figure 2.1(b), it can be seen that a slightly banded structure (i.e. pearlite-rich bands aligned along the rolling direction) is visible through the thickness of the plate.

[1] Centre R&D du Groupe Cockerill-Sambre, Boulevard de Colonster B57, Sart Tilman, 4000 Liège.

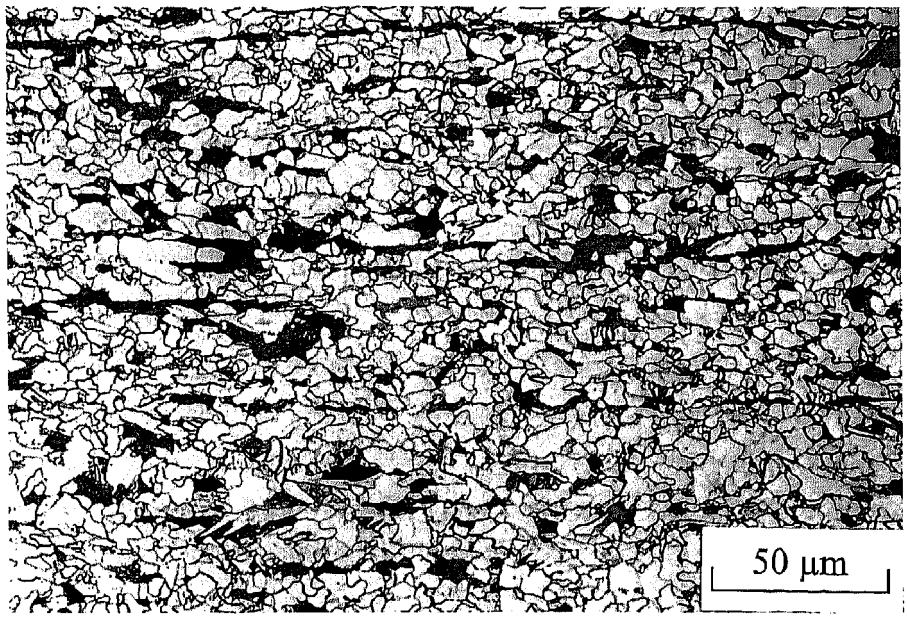

(a)

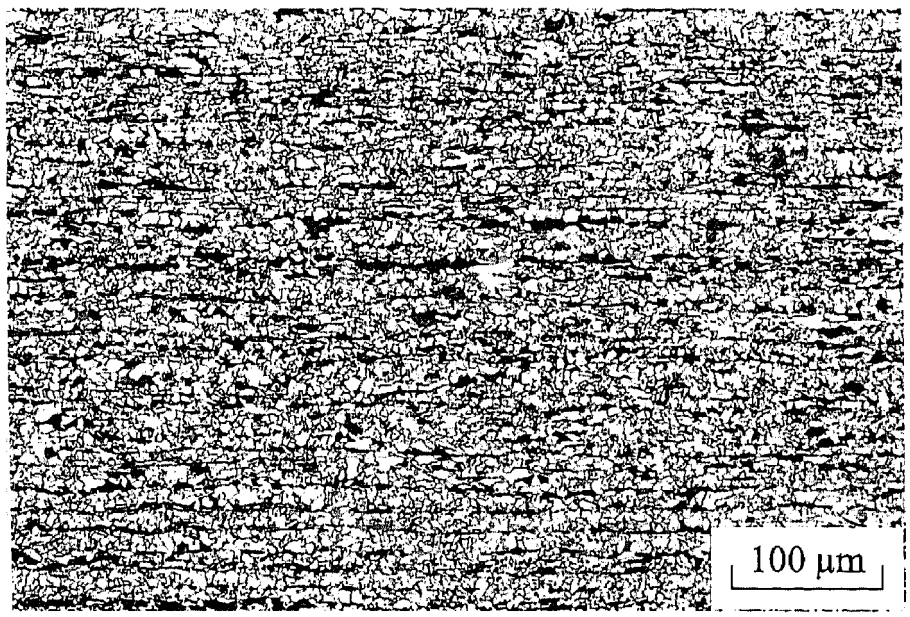

(b)

Figure 2.1: Light micrographs of the as hot-rolled microstructure of steel LSi (2% Nital etched). Microstructure consists of ferrite and pearlite (a). A slight banded structure in the rolling direction is visible through the thickness of the plate (b).

Because of their high silicon contents, steels HSiI and HSiII cannot be industrially produced[2]. Alloys HSiI and HSiII were therefore laboratory produced by vacuum melting and casting as 100kg ingots[3]. Both ingots were then hot-rolled following conditions near classical industrial practice[4]. Each ingot was first reheated to 1250°C for 1 hour. Roughing was then conducted at temperatures higher than 950°C down to a thickness of 20mm. This thickness was then reduced to 4mm in 5 passes. Coiling was finally simulated by placing the hot-rolled plates for 1hour in a furnace and by then allowing furnace cooling to room temperature. The same hot-rolling scheme was conducted on a small piece of steel HSiII with larger thickness at each stage of rolling and a final thickness of 15mm. This plate was cold-swaged in such a way as to obtain cylinders for dilatometric measurements. Since it is generally admitted that coiling at relatively high temperature enhances the banded structure when silicon and manganese contents are large, simulated coiling was conducted at 550°C and 620°C for steels HSiI and HSiII, respectively. Figure 2.2 presents the resulting microstructures. As shown in figures 2.2(a) and 2.2(c), owing to the low coiling temperature, pearlite has been replaced by upper bainite, bringing about a very fine distribution of cementite. For steel HSiI, the microstructure is therefore constituted by a mixture of ferrite and upper bainite while for steel HSiII, the higher carbon content brings about a fully bainitic microstructure. Furthermore, figures 2.2(b) and 2.2(d) show that no banding can be found in both steels.

[2] These high silicon levels incompatible with the present industrial practice can be considered as the major drawback for the industrial development of these TRIP-assisted multiphase steels.

[3] Ingot of steel HSiI was supplied by CRM, Rue E. Solvay 11, B-4000 Liège, Belgium while ingot of steel HSiII was supplied by British Steel, Swinden Technology Centre, Moorgate, Rotherham, South Yorkshire, England, S60 3AR.

[4] Hot-rolling was conducted on laboratory installations of CRM, Hall de Métallurgie, Sart Tilman, 4000 Liège, Belgium.

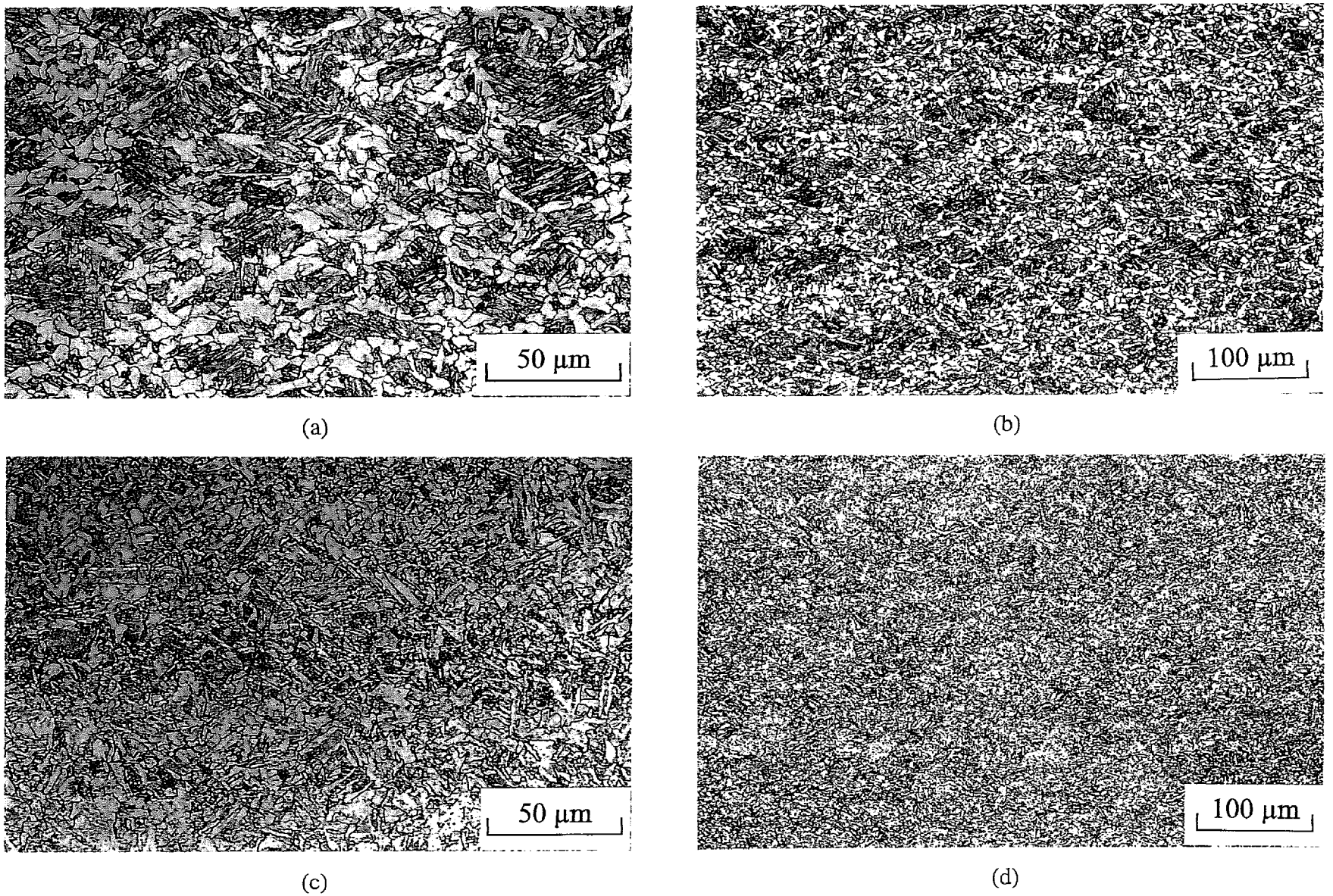

Figure 2.2: Light micrographs of the as hot-rolled microstructures of steels HSiI ((a) and (b)) and HSiII ((c) and (d) (2% Nital etched). Microstructure of steel HSiI consists of ferrite and upper bainite (a) while only upper bainite is found in steel HSiII (c). No banding can be observed in both steels ((b) and (d)).

Cold-deformation, principally cold-rolling, was finally applied to each hot-rolled plate. Steel HSiI and HSiII were cold-rolled 75% to 1mm in thickness while hot-rolled plates of steel LSi were cold-rolled 82% to the same thickness of 1mm. For the dilatometric measurements requiring cylindrical hollow samples, cold-swaging was applied on cylinders machined from the hot-rolled plates. Similar cold-deformation level as for the cold-rolling was applied on steel HSiII while cold deformation was slightly smaller for steel LSi. These cold-deformed sheets or cylinders of each steel grade constituted the raw material of the different studies carried out in this thesis.

2. Experimental Procedures

2.1. Thermal processes

After cold-rolling, the specimens had to be heat-treated in order to generate the required multiphase microstructure. As reminded in figure 2.3, in the case of cold-rolled samples, the particular microstructure of the TRIP-assisted multiphase steels is obtained at the end of a 2 isothermal stage heat-treatment. The samples are first reheated between Ac_1 and Ac_3. During this ***intercritical annealing***, part of the microstructure transforms into austenite. The samples are then rapidly cooled to an intermediate temperature situated in the ***bainite transformation*** temperature range for a second isothermal holding. They are finally quenched to room temperature. The heat-treatment conditions are defined by several parameters. Among them, the temperatures and times of the 2 dwells as well as the cooling rate between the dwells are certainly key factors which must be precisely controlled.

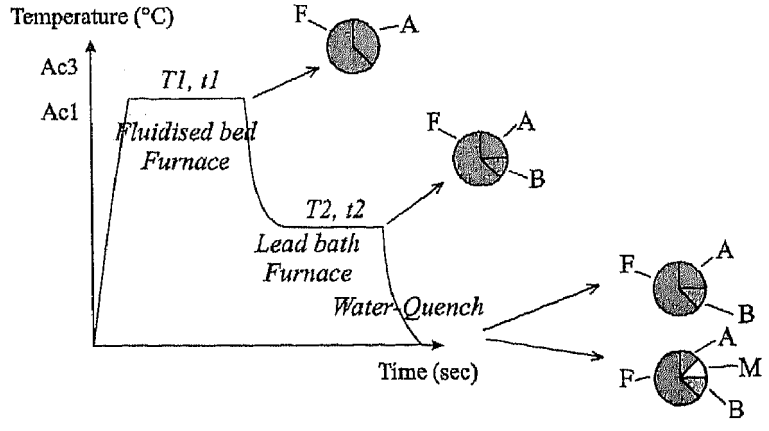

Figure 2.3: Schematic illustration of the heat-treatment needed for the generation of cold-rolled TRIP-assisted multiphase steels.

2.1.1 Heat-treatment of cold-rolled steel sheets

Heat-treatments were carried out on large samples by making use of 2 conduction furnaces. The samples were first intercritically annealed in a fluidised bed furnace. This furnace is constituted by a resistively heated crucible (ø 200mm x 350mm) filled up with alumina powder (ø ~ 400µm). Injected air fluidises this powder in such a way that high heating rates, good temperature homogeneity and stability are insured. For the bainitic tempering, a high cooling rate from the intercritical range and an adequate temperature stability were insured by immersion in a lead bath furnace constituted by a crucible (ø 120mm x 340mm) filled with lead. In order to avoid lead adhesion, boron nitride was sprayed on the samples prior to heat-treatment. The samples were finally water quenched. Figure 2.4 presents the measured temperature as well as the heating and cooling rates obtained with our set-up during a typical heat-treatment. This installation thus allows setting 4 parameters, i.e. the temperatures and times of the intercritical annealing and of the bainitic tempering. The heating and cooling rates were fixed by the heat transfer between the baths and the samples. For the intercritical annealing, heating rate was around 50°C/s. The mean cooling rate between the 2 isothermal holding stages was around 70°C/s with a peak value of 140°C/s. These values are in good agreement with published results and it will be shown that they allow the formation of the desired microstructures. Temperatures fluctuations during the isothermal holdings were of the order of 2°C.

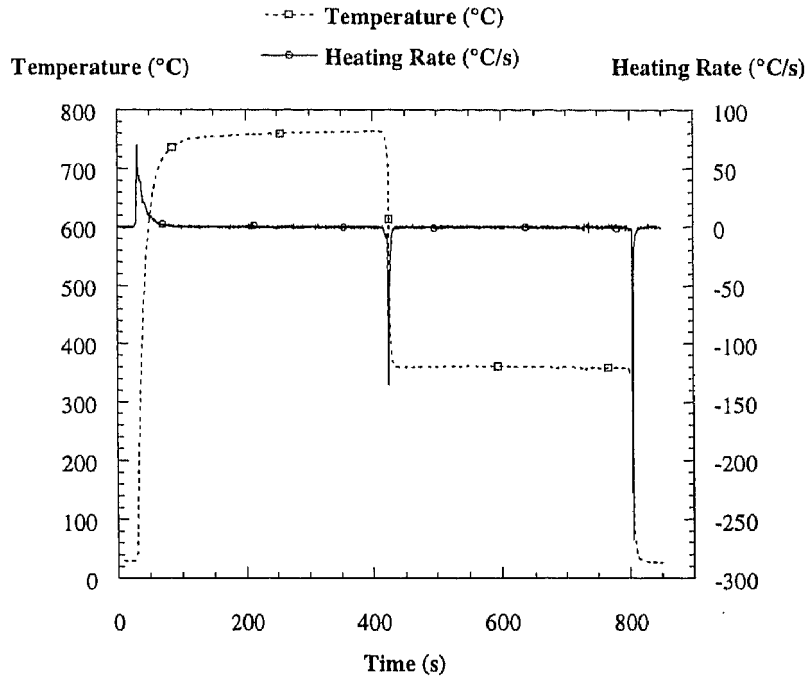

Figure 2.4: Evolution of the temperature during a typical thermal cycle as well as heating and cooling rates obtained with the experimental installation.

2.1.2 Simulation of heat-treatment in a quench dilatometer

In order to follow the bainite transformation kinetics, some heat-treatment were simulated in a quench dilatometer using hollow cylinders,. Two different experimental installations were used. Heat-treatments were first conducted on a BÄHR-Thermo-Analyse quench dilatometer allowing fast heating and cooling rates thanks to inductive heating and cooling by high pressure helium gas spray. The cooling rate between the 2 isothermal holding was set up at 75°C/s. The specimens were 10mm long and presented external and internal diameters of 4 and 3.75mm respectively. For steel HSiII, heat-treatments were also conducted in a modified ADAMEL Ditirc quench dilatometer for holding times at the bainitic tempering temperature which were sometimes longer than 1 day. In this case, 30mm long samples (with external and internal diameters of 4 and 2.8mm respectively) were placed inside of a vertical quartz tube. Another quartz tube with the same diameter as the sample was used to transmit sample elongations to the LVDT. The tube containing the sample and the LVDT could then be moved rapidly between different lead bath furnaces for the successive isothermal holdings. The experiments were carried out under helium atmosphere in order to accelerate the heating and cooling rates of the sample. This system allowed a mean cooling rate between the 2 isothermal holdings of 35°C/s with a peak value of 85°C/s. This installation was validated and calibrated on samples of high purity Nickel and AISI 304L austenitic steel.

2.2 Investigation of the mechanical properties

Different experimental procedures were used in order to test the mechanical properties of the TRIP-assisted multiphase steels. Uniaxial tensile testing was mainly used but other tests were also carried out as described hereafter.

2.2.1 Tensile testing

Tensile specimens were prepared according to the European standard EN 10002-1 represented in figure 2.5 with the tensile axis parallel to the rolling direction[5]. The initial gauge length was 50 mm and the width was 12.5 mm. Tensile testing was done at a crosshead speed of 2mm/min[6]. Measured loads and elongations were converted to true

[5] This geometry as well as the other geometries described hereafter were machined by spark erosion which ensures no prior deformation and a perturbed zone size of only a few micrometers.

[6] This crosshead speed corresponds to a mean deformation rate of 2.7 10^{-4} s^{-1} on a large part of plastic straining. Furthermore, tensile testing carried out on the same TRIP-aided steel at crosshead speeds varying

stress - true strain curves. Yield strength (σ_y), true stress at maximum load (σ_{TS}) and true uniform strain (ε_u) (i.e. the maximum uniform true strain) were measured from these tensile curves. The yield strength was defined either as the conventional 0.2% yield strength ($\sigma_{0.2}$) or as the true stress corresponding to the Lüders deformation plateau for samples with continuous or discontinuous yielding behaviours, respectively.

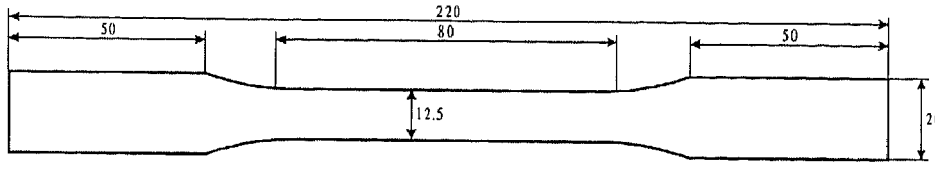

Figure 2.5: Geometry of the tensile specimens machined according to the European standard EN 10002-1.

It is well known that the strain hardening behaviour of Dual Phase steels and TRIP-aided steels cannot be described by classical expressions such as the Hollomon equation or the Crussard-Jaoul equation [Jian92, Reed73]. Strain hardening was therefore described using the incremental strain hardening exponent ($n_{incr.}$) proposed by Sachdev [Sach83] for Dual Phase steels. This exponent corresponds to the slope of the line fitting the logarithmic plot of the true stress - true strain curve for a given increment of the strain (a strain increment of 0.003 was chosen). An incremental strain hardening exponent curve covering the entire uniform deformation range is obtained in this way.

2.2.2 Tensile testing at various temperatures

Isothermal tensile tests were performed at temperatures between –30°C and 120°C[7] on tensile specimens prepared according to the same European standard EN 10002-1 (figure 2.5). The tests were carried out in a closed chamber resistively heated or cooled by expansion of pressurised CO_2. A thermocouple was spot-welded at the end of the calibrated zone of each specimen in order to monitor temperature during tensile testing. The chamber was set at the test temperature prior to mounting the sample on the grips in order to minimise (and to keep constant) the time of exposition of the specimens at each temperature. Tensile tests were carried out at a crosshead speed of 2mm/min. In this case,

---

from 0.2mm/min to 200 mm/min showed that the strain rate dependence of the steel properties was not too large in this range of deformation rate.

[7] The upper limit of the temperature range for this study corresponds to the beginning of dynamic strain aging which leads to inhomogeneous deformation (characterised by serrated flow) and therefore shows an extreme sensitivity to temperature and strain rate.

the initial gauge length of the analogic extensometer was 25mm. The same parameters as in the case of the room temperature tests were obtained from the measured loads and elongations. Flow stresses at different strain offsets prior to the Lüders plateau (from 1.10^{-4} to 4.10^{-4}) were measured from the true stress – true strain curves at each temperature by considering the intercepts of the stress-strain curves with straight lines parallel to the elastic loading line.

2.2.3 Microindentation Vickers hardness

Microindentation Vickers hardness measurements of the idiomorphic ferrite matrix were carried out on some samples. Because of the small grain size of ferrite (~5-10μm), loads of 1 and 2g were chosen in order to keep the indentation size small enough in comparison to the grain size. Prior to these tests, the samples were mechanically polished to 0.25μm diamond paste and then electrolytically polished for 10min in a solution of 5% $HClO_4$ and 95% glacial acetic acid in order to remove any work hardened surface layer. They were finally etched with 2% Nital for revealing the different phases. After indentation, the diagonals and area of the impressions were accurately measured by scanning electron microscopy (SEM). These measurements were calibrated by carrying out the same indentation tests with 1 and 2g load on standards whose hardness under 10g is known.

2.2.4 Characterisation of damage and fracture toughness

In order to characterise the coupling between the TRIP effect and damage/fracture properties, tensile tests were carried out on notched specimens The geometry is represented in figure 2.6. Specimens were strained to various levels of average deformation, $\varepsilon_{aver}=\ln(S_0/S_f)$ (where S_0 and S_f are the initial and final minimum sections, respectively), and then unloaded for systematic metallographic observations. S_f was obtained by measuring the final ligament length using a travelling microscope and the final ligament thickness at various locations along the ligament length using a profilometer.

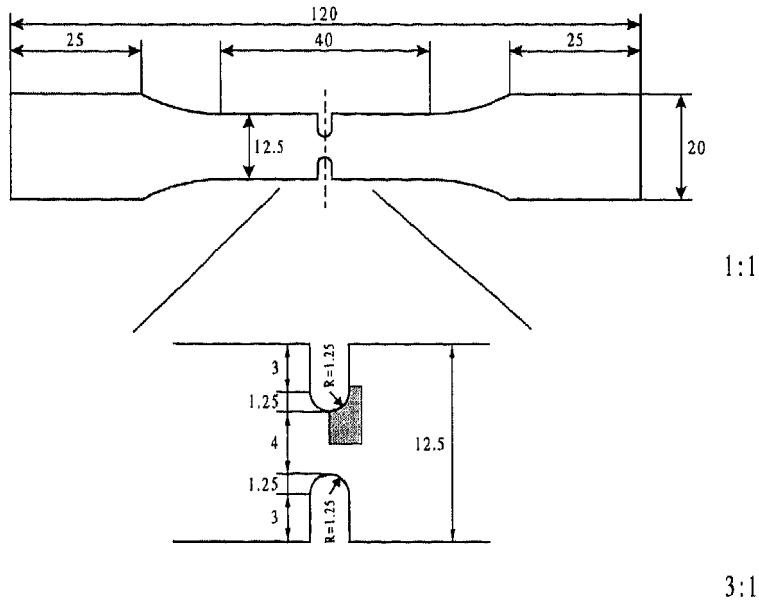

Figure 2.6: Geometry of the notched specimens used for the characterisation of damage and martensitic transformation.

For the evaluation of fracture toughness, the DENT geometry schematically represented in figure 2.7 was used. The specimens width, w, was 55mm and the thickness, t_0, was 1 mm. Precracking of the specimens was carried out by fatigue using a servo-hydraulic INSTRON testing machine. The initial notches were machined by spark-erosion followed by tracing the tip with a razor blade in order to favour rapid initiation of the fatigue precrack. In order to obtain 2 mm long fatigue cracks on both sides of each specimen and to conserve a symmetric configuration, we clamped the side at which the fatigue crack length first attained 2 mm and further carried on cyclic loading until the second fatigue crack reached also 2 mm length. The maximum applied load was chosen in such a way that the maximum stress intensity factor during precracking never exceeded 20% of the expected fracture toughness of the plate (which was verified a posteriori). The ratio a/w after precracking was always close to 0.5. The width zone along the crack sides where martensitic transformation had occurred during fatigue precracking was measured by SEM observation and found to be equal to 30 μm for steel HSiII and 40 μm for steel LSi.

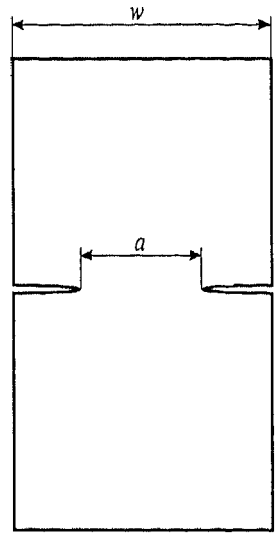

Figure 2.7: Geometry of the DENT specimens used for the toughness measurements.

The precracked DENT specimens were loaded in tension. The tests were interrupted at various load levels (multiple-specimens method). In order to characterise the cracking resistance by JR curves, the J integral [Rice68] and the crack advance, Δa, are determined for each specimen. J was computed from the load/displacement curve using the formula of Rice *et al.* [Rice73] for the DENT:

$$J_{Rice} = \frac{K_I^2}{E} + \frac{1}{l_0 t_0}\left(2\int_0^{U_p} P(u_p)du_p - PU_p\right)$$

where K_I is the mode I stress intensity factor, E is the Young's modulus, P is the applied load, u_p is the plastic displacement and U_p is the maximum plastic displacement. No correction for crack advance was made. Δa was measured on polished section on both sides of the specimens. In order to account for tunnelling effect, measurements were performed on the surface, at quarter thickness and at mid thickness. Δa was averaged on both sides of the specimens for all the through thickness measurements. The resistance to crack propagation is characterised by the tearing modulus defined as :

$$T_R = \frac{E}{\sigma_0^2}\frac{dJ_R}{da}$$

where E is the Young's modulus, σ_0 is the yield strength and a is the crack advance.

Both tests were also numerically simulated by the finite element method[8]. The particular numerical procedures are described in chapter VII.

[8] These simulations were carried out by Dr. Th. Pardoen, present address: Division of Engineering and Applied Sciences, Harvard University, Pierce Hall 314, Cambridge 02138, USA.

2.3 Characterisation of the microstructure

The drastic influence of microstructure on physical and mechanical properties of steels makes metallographic examination a necessity for the understanding and enhancement of properties. We devoted much work to reveal the complex microstructure of the TRIP-assisted multiphase steels. New metallographic methods have been designed[9]. On the other hand, a complete characterisation of retained austenite was found essential. For this purpose, we made wide use of Mössbauer spectroscopy and x-ray diffraction.

2.3.1 Metallographic methods for revealing the microstructure of TRIP-assisted multiphase steels

In order to reveal specific microstructural characteristics, numerous etching methods have been developed in the literature among which chemical etching is certainly the easiest and the most widely used. This technique consists in a controlled corrosion process driven by the heterogeneity of the electrochemical potential between surface areas with different chemical or physical properties [Vand84a]. Etching induces the selective dissolution or preferential staining of the phases. However, classical etching techniques used for the investigation of steel microstructures allow the simultaneous observation of only a restricted number of phases. So far, this limitation was not too detrimental since most low carbon steel grades possess a relatively simple microstructure.

Beside the general steel etching solutions such as nital (solution of nitric acid in ethyl-alcohol which outlines ferrite and ferrite-cementite grain boundaries), a large number of other reagents has been developed [Vand84b, Ray96] for emphasising specific microstructural features. Examination of nital etched Dual-Phase steels by light microscopy was generally not found satisfactory since these steels exhibit little post nital etching contrast. This led to the development of new tint etchants [Vand84c] which allowed easy distinction by colouring one or both phases.

Observation of the microstructure by scanning electron microscopy (SEM) using secondary electrons contrast requires first the creation by etching of a topographic contrast between the different phases. Nital is generally well adapted, since it etches preferentially ferrite while leaving intact austenite and cementite. The etching of ferrite-based phases

[9] The development of metallographic methods was carried out in collaboration with E. Girault, Department of Metallurgy and Materials Science, K.U.Leuven, de Croylaan 2, B-3001 Leuven, Belgium. The results have already been published: E. Girault, P. Jacques, Ph. Harlet, K. Mols, J. Van Humbeeck, E. Aernoudt and F. Delannay, *Mater. Charact.*, 1998, vol. 40, pp. 111-118

such as bainitic ferrite and pearlitic ferrite provides a typical morphology which generally allows recognition of these phases. The situation becomes more complex when a microstructure presents simultaneously austenite and martensite as second phases. In this case, the usual slight nital chemical etching is not selective enough for allowing distinction between the two phases. On investigation of Dual-Phase steels, this limitation was never critical since austenite was not considered a major phase of the microstructure.

In summary, the existing etching techniques for light microscopy as well as for SEM were not found satisfactory. New procedures were therefore developed in order to allow the simultaneous observation of the 4 phases constituting the fine-grained microstructure of the TRIP-assisted multiphase steels.

For observations by light microscopy, a colour etching technique was adapted from the LePera method [Lepe80] and developed to reveal the microstructure of multiphase steels. The specimen is embedded in an acrylic resin that stiffens at room temperature. The classical grinding and polishing stages are performed at least down to the use of 1μm diamond paste. After each sequence of polishing, the specimen is rinsed only with ethanol in order to avoid any risk of oxidation. It is then dried under a warm air flow.

The etchant is a mixture of two pristine solutions whose compositions are: (i) 1g of $Na_2S_2O_5$ in 100ml distilled water; and (ii) 4g of picric acid in 100ml ethanol. Volumes of 10ml of each reagent are mixed in a small crystallising vessel just before starting etching. The specimen is immediately immersed horizontally in the mix. It is given a permanent oscillation during the whole etching time which lasts between 45 and 75 seconds, depending on the steel composition. After etching, the sample surface is immediately flushed with water and then ethanol and blown dry under a cool air flow. The sample is finally observed in a microscope equipped with a high brightness halogen lamp.

SEM samples preparation involved polishing till sub-micron diamond suspension. Specific care was taken during final cleaning: the use of water-free cleaning media is strongly recommended in order to avoid any corrosion phenomenon typical of high Si bearing steels. Specimens were then etched with a 2% nital solution for times ranging from 10 to 15 seconds.

2.3.1.1 As-annealed TRIP-aided steels

The tint etching procedure was applied to each steel grade. The micrograph of figure 2.8 illustrates the microstructure of steel HSiII in which ferrite appears in blue, bainite in

brown and both retained austenite and martensite in white. A comparison of the micrographs on figures 2.8 and 2.9 (presenting the microstructure of steel LSi) illustrates how the chemical composition of the steel affects the intensity of the colours. A highly alloyed steel (figure 2.8) exhibits more contrasted tints. Carbon and silicon contents have a substantial influence on the colour of the ferritic matrix. It can be observed on these figures that ferrite turns from blue to brown when decreasing the content of carbon and silicon. The only drawback of this method is the impossibility of distinguishing retained austenite from martensite since both appear white.

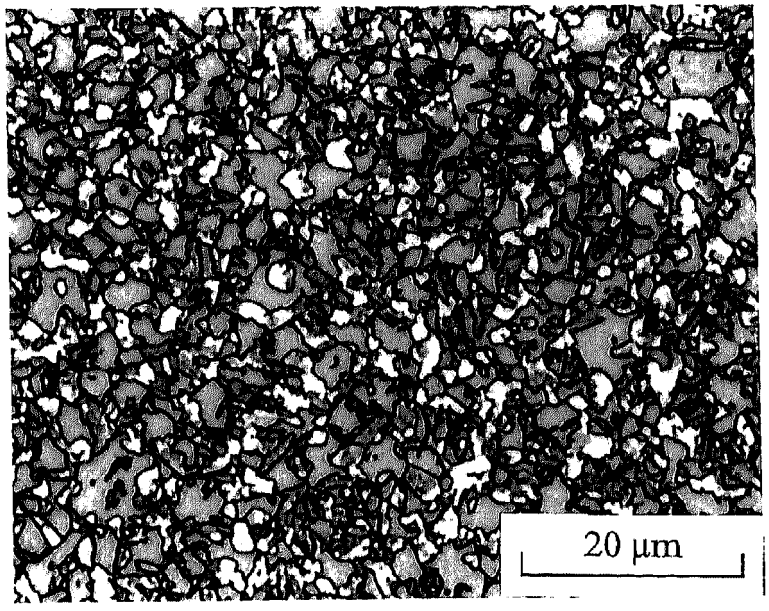

Figure 2.8: Light micrograph of typical as-annealed steel HSiII microstructure after tint etching adapted from the LePera technique (idiomorphic ferrite in blue, bainite in brown and martensite/austenite in white).

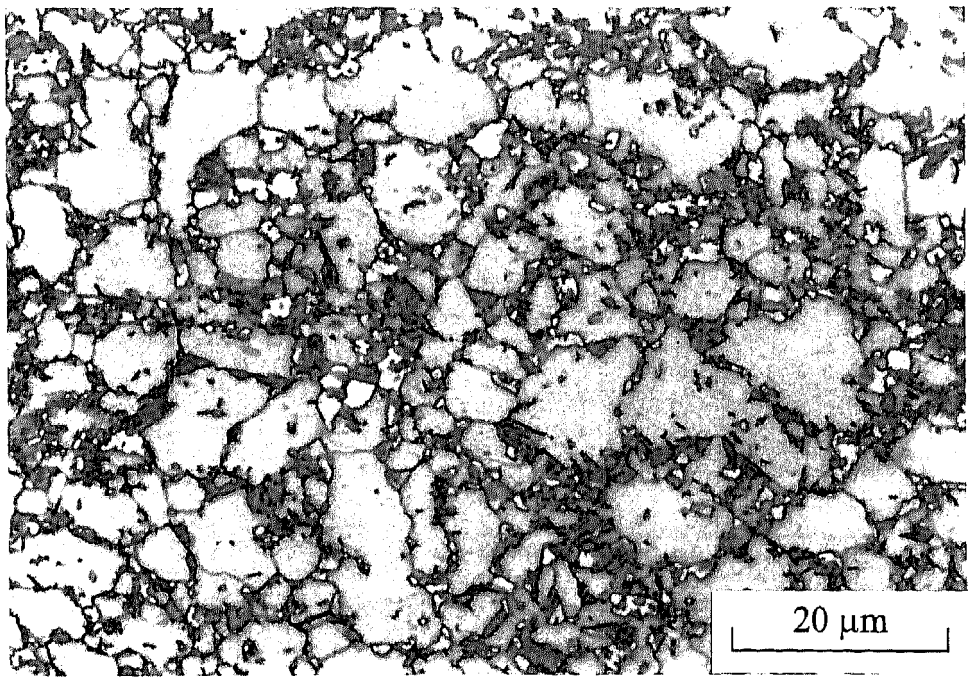

Figure 2.9: Light micrograph of typical microstructure of steel LSi after tint etching adapted from the LePera technique. In this case, idiomorphic ferrite matrix appears pale brown.

This lack of distinction of retained austenite and martensite remains when TRIP-assisted steels are examined by SEM. Figure 2.10 exhibits micrograph of a sample processed using a short ageing time in such a way as to insure the presence of martensite among the microconstituents. This micrograph clearly shows that the applied etching time allows easy identification of the microstructure characteristics, except for martensite and retained austenite which cannot be separately identified. As shown in Figure 2.11, a deeper etching of 90 seconds may indeed reveal some substructure in martensite but the other phases become overetched and thus unrecognisable. Hence, it seems that all constituents of the microstructure cannot be characterised by only the use of chemical etching since a common time revealing all phases can not be found.

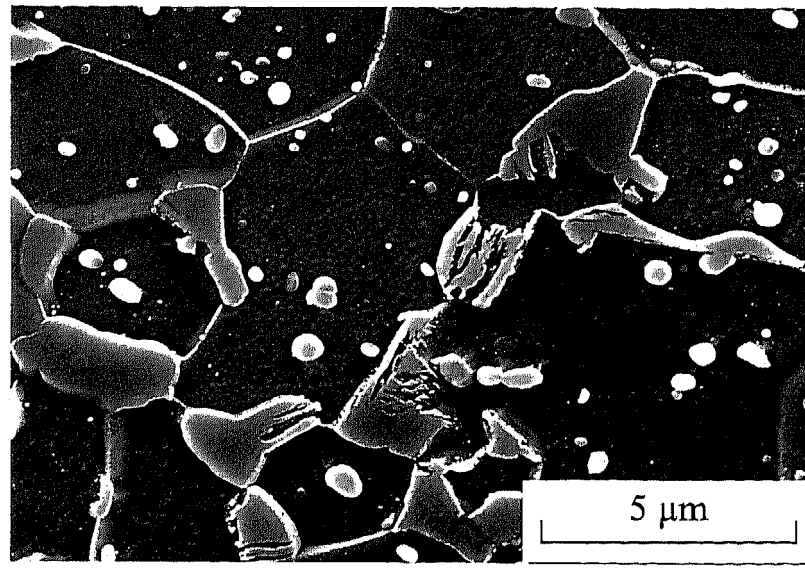

Figure 2.10: SEM micrograph of nital-etched heat-treated steel HSiII. Retained austenite and martensite exhibit both a smooth and featureless aspect.

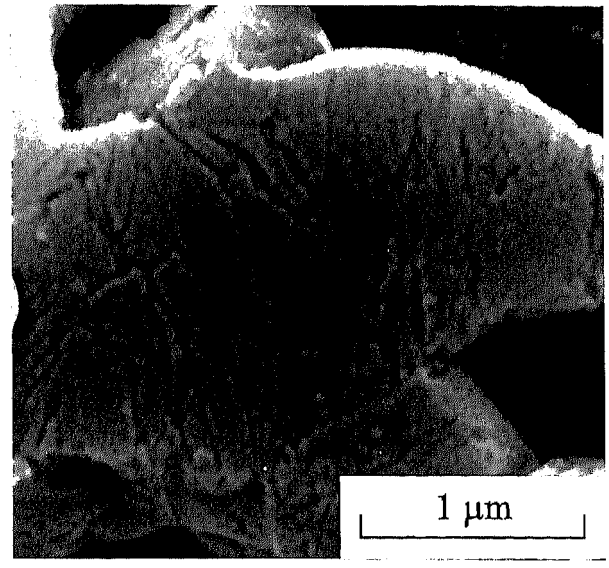

Figure 2.11: SEM micrograph of overetched heat-treated steel HSiII, denoting a slight substructure on a martensite grain.

2.3.1.2 Tempered TRIP-aided steels

Darkening of martensite by tempering followed by nital etching is a common technique to facilitate light microscopy examination [Spei81b]. This method is well adapted for simple microstructures but can lead to erroneous identifications when multiphase TRIP-aided steels are considered: ferrite and austenite appear bright whereas bainite and martensite are both dark coloured. However, the proposed tint etching method was attempted on tempered

specimens in order to check whether a sufficient colour contrast can be obtained to allow recognition of all involved microconstituents. Figure 2.12 shows the microstructure of steels LSi and HSiII tint etched after tempering for 2h at 200°C. The tempering treatment does not appear to have influenced the original colour range. The ferritic matrix remains blue-brown whereas retained austenite islands (on which tempering has no effect, as shown hereafter) remain white. The ferritic bainite, whose morphology is easily distinguishable, presents a dark brown colour. The new feature is the appearance of an additional light brown tint visible on coarse second phase grains. Since slight tempering affects neither ferritic phases [Spei81a] nor retained austenite, these off-white grains are identified as martensite. This will be confirmed from SEM observations.

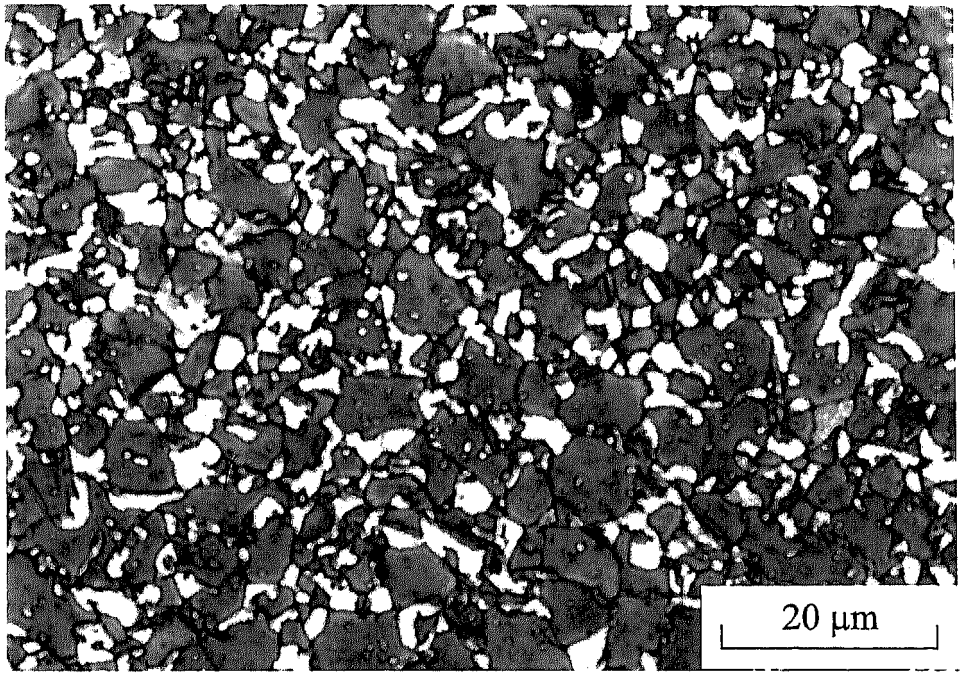

(a)

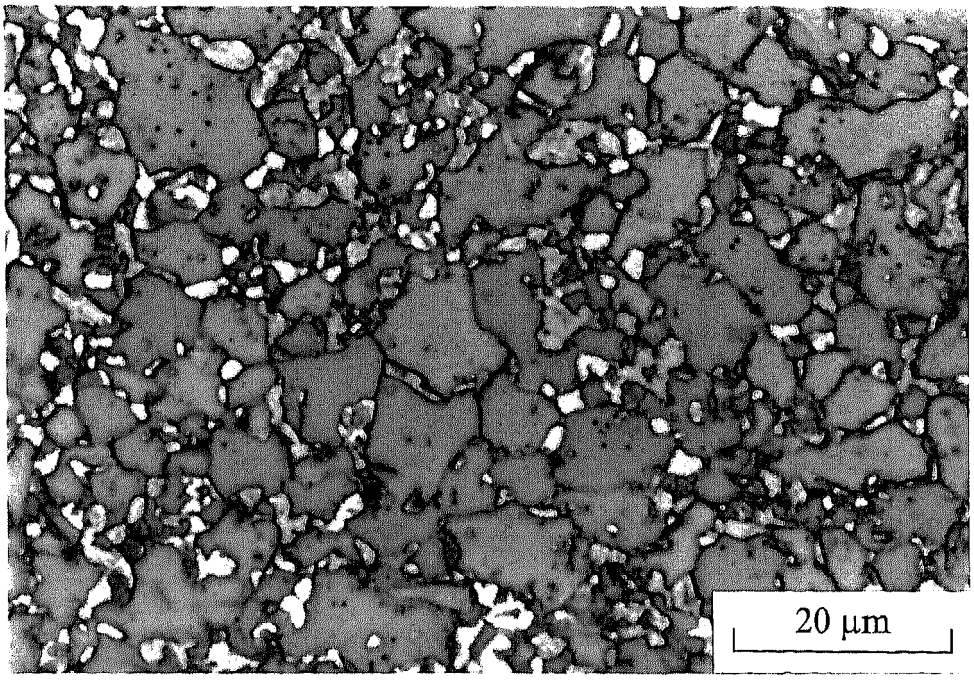

(b)

Figure 2.12: Light micrographs of tempered and tint etched steels HSiII (a) and LSi (b). Martensite grains can be recognised by their off-white colour.

Comfortable observation of the multiphase microstructure of the TRIP-aided steels requires the use of SEM after tempering for 2 hours at 200°C and standard sample preparation with nital etching. Micrographs of figure 2.13 show that martensite can then be distinguished from retained austenite as a result of a very fine etching of the martensite grains. The emergence of the martensite substructure can be interpreted as resulting from carbide precipitation during tempering [Spei92]. These carbide precipitates are sensitive to etching. During tempering between 100 and 200°C, ε-carbides precipitate in martensite. Holding in this temperature range (the so-called first stage of tempering T1) results in a dispersion of coarse particles within low-carbon martensite grains. Since this precipitation preferentially occurs at interlath or interplate boundaries [Spei92], a subsequent etching leads finally to the resolution of the martensite substructure.

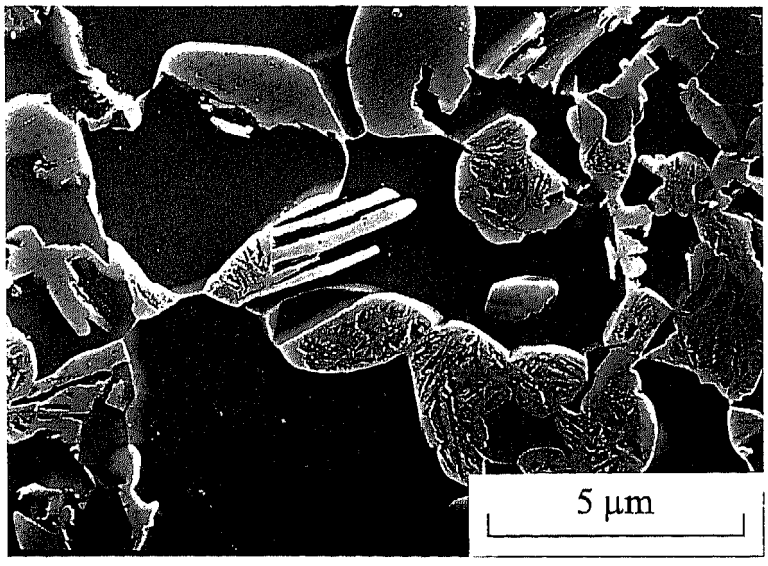

(a)

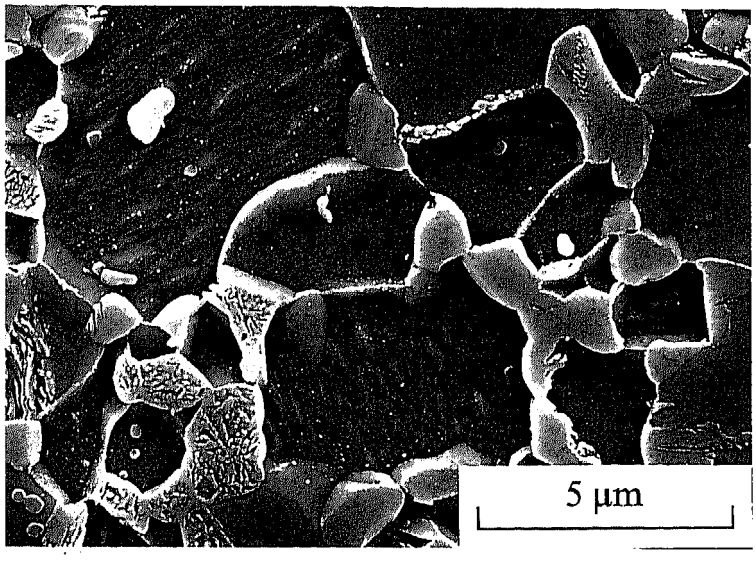

(b)

Figure 2.13: SEM micrographs of the heat-treated, tempered and nital etched samples of steel HSiII (a) and LSi (b). Martensite can be easily distinguished from austenite thanks to the emergence of its substructure.

The 2 hours tempering treatment followed by nital etching was found to lead to a good resolution of the martensite substructure and therefore to an easy distinction of martensite and retained austenite. Moreover, it was shown that this tempering treatment has no influence on the austenite content.

Therefore, it can be concluded that the proposed tempering treatment (200°C for 2h) is a good procedure to allow the observation of martensite in TRIP-aided steels without leading to any major alteration of the other phases present in the microstructure.

2.3.2 Characterisation of the retained austenite of TRIP-assisted multiphase steels

In order to precisely characterise the influence of the thermal treatment on the retention of austenite and the influence of the mechanically-induced martensitic transformation on the mechanical properties of the TRIP-aided steels, it was of primary importance to measure the variation of austenite volume fraction and austenite carbon content during thermal treatment and during tensile testing. Particular care was thus devoted to the accurate measurement of these parameters.

2.3.2.1 Measurement of retained austenite volume fraction by Mössbauer spectroscopy

In the published literature on TRIP-aided steels, x-ray diffraction is commonly used for the measurement of the retained austenite volume fraction. However, the relationship between austenite volume fraction and the intensities of the diffracted peaks of ferrite and austenite is not straightforward when preferential crystallographic orientations exist. In fact, as a result of hot- and cold-rolling, these steels are textured and the use of x-ray diffraction for the measurement of phase volume fractions must be considered with particular care. Two techniques are commonly recommended [Jatc80]: (i) artificial reconstruction of a non-textured sample by rotating and tilting the sample during measurement; (ii) averaging the intensities by using as many diffraction peaks as possible.

In the present case, we used a technique insensitive to the texture of the samples, i.e. the ***Mössbauer spectroscopy***. We will first briefly explain the underlying physical principles of the method and explain afterwards how the method can be used for the determination of the retained austenite contents.

a) The Mössbauer effect – Recoilless γ-ray nuclear transition

The resonance absorption of a radiation is a phenomenon well known in many branches of physics[10]. It might be thought that the same phenomenon should occur for the γ-radiation emitted when nuclei in excited states release their excess energy by emitting a radiation. However, because of the much higher energy of γ-rays, the effect of the recoil momentum (conservation laws) which can be neglected in other cases of resonance, becomes dominant

[10] The scattering of sodium light by sodium vapour or the excitation of a dipole by a radio-frequency radiation are some familiar examples.

for γ-radiation. As a consequence, recoil energy prevents the observation of nuclear resonance absorption by *free atoms*.

The Mössbauer effect arises when *emitting atoms are bound in a crystal* in such a way that they are no longer able to recoil individually. In a quantum mechanical description, the physical origin of the Mössbauer effect, i.e. of the possibility of momentum transfer without energy transfer, lies in the discrete nature of lattice vibrations. The recoil energy is lower than the energy of lattice vibrations (phonons). It turns out that the recoil phenomenon involves the excitation of N atoms together so that the recoil energy to be absorbed is 'diluted' and therefore does not prevent the nuclear resonance absorption.

b) Mössbauer spectroscopy

The Mössbauer effect thus enables the resonant absorption of γ-rays to be observed. Furthermore, this Mössbauer effect makes possible the observation of small shifts or splittings of the energy levels of nuclei in solids, the *hyperfine interactions*. These interactions may be regarded as resulting from small additional static interactions which occur between a nucleus and its environment as a consequence of the fact that a nucleus is not a structureless point charge, but a cluster of moving charges distributed over a finite volume. The Mössbauer effect provides a very detailed account of the way in which a nucleus interacts with its environment. However, if the emitting nucleus is in a different environment than the receiving nucleus, the resonance may be destroyed. A convenient way to scan the influence of the extra-nuclear environment of a nucleus exhibiting a Mössbauer effect is to slightly change the energy of the radiation emitted by the source by using the Doppler effect. A range of energy around the 'natural' energy transition is therefore scanned by imparting known velocities to the source. Three types of hyperfine interactions can therefore be observed:

- *The monopole interaction or isomer shift*: This shift is proportional to the difference of the electron density at the nuclear site between the source and the analysed compound. Changes of valency, or of electron configuration which involve changes in the total number of *s* electrons, will usually be accompanied by significant changes of the isomer shift.
- *The quadrupole splitting*: The quadrupole splitting occurs when the nuclear charge is not spherically distributed. It results from the interaction between a nuclear quadrupole and an electric field gradient. An electric field gradient will be generated at the nucleus whenever the nuclear environment has a charge symmetry lower than cubic. This

interaction does not affect the ground state but removes the degeneracy of the upper state.

- *The magnetic splitting*: When the nucleus contains magnetic dipole moments, these dipoles will interact with any magnetic field (either internal or external). A Mössbauer type transition inevitably involves a change in the nuclear spin-state. It therefore follows that at least one of the nuclear state involved will have non-zero spin. A strong enough magnetic field will therefore always cause splitting in a Mössbauer spectrum (following transition rules, 6 transitions are allowed).

These 3 types of hyperfine interactions are schematically represented in figure 2.14 as well as the corresponding Mössbauer spectra.

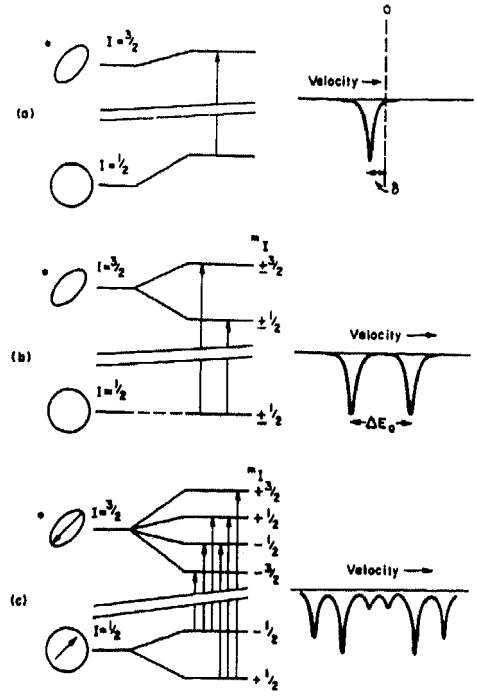

Figure 2.14: Schematic illustration of the hyperfine interactions. On the extreme left of each diagram are shown the unperturbed nuclear levels, the I=3/2 state being 14.4KeV above the I=1/2 ground state (from [Cran85]).

c) Mössbauer spectroscopy of TRIP-assisted multiphase steels

Several studies [Chri68, Gen68, Abe74, Azev78, Cran85, Ladr86, Maur86] have shown that Mössbauer spectroscopy is a powerful tool for the characterisation of some features of the microstructures of heat-treated steels. The measurement of retained austenite volume fractions is allowed since ferrite-based phases, i.e. ferrite, bainitic ferrite and martensite, are ferromagnetic and bring about a magnetic splitting while austenite is paramagnetic.

The measurements were carried out following a conventional transmission technique[11]. Samples (~ 1.5 x 1.5 mm^2) were first chemically thinned to a thickness of 100µm by using a solution made of 14ml of HF and 100ml of 30% H_2O_2 diluted in 100ml distilled water. They were then electrolytically polished in a solution of 5% $HClO_4$ and 95% glacial acetic acid to a thickness of 30 to 50µm. The source was a conventional radioactive ^{57}Co source. For sufficient precision, a minimum of 10^6 hits was measured for each sample. Typical spectra are presented in figure 2.15. These spectra have been least-square fitted with Lorentzian peaks. On figure 2.15(a), it can be seen that the fitting of the experimental data assumes the presence of retained austenite (the central singlet) and 2 different ferromagnetic configurations. They correspond to environments of iron atoms of ferrite-based phases with 0 and 1 nearest neighbour different of Fe (i.e. Mn or Si) respectively. In the case of samples with large amounts of carbon rich austenite (such as in the case of steel HSiII – figure 2.15(b)), a supplementary doublet was added to the fitting. In this case, the paramagnetic singlet is associated with iron atoms in austenite remote from carbon atoms whereas the doublet due to a quadrupole effect, represents absorption by iron atoms in austenite having 1 carbon atom as nearest neighbour on interstitial sites. Indeed, the carbon atoms in the austenite destroy the strict cubic symmetry of the FCC structure, and produce an electric field gradient at their neighbours iron atoms. These atoms therefore show a doublet superimposed on the singlet of the austenite line.

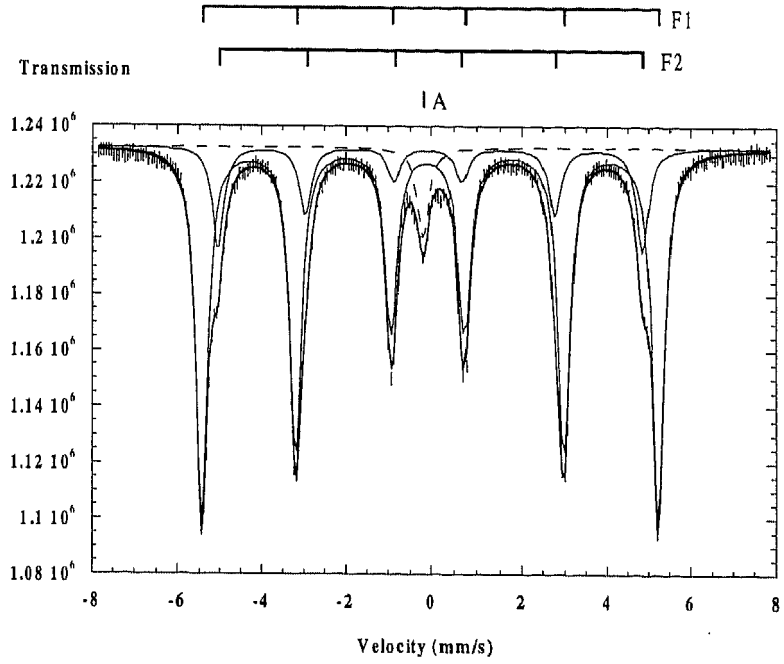

(a)

[11] All the measurements have been carried out at UCL, Laboratoire de chimie inorganique et nucléaire, Chemin du cyclotron 2, B-1348 Louvain-la-Neuve, Belgium. We are grateful to Prof. J. Ladrière for the provision of the experimental facilities.

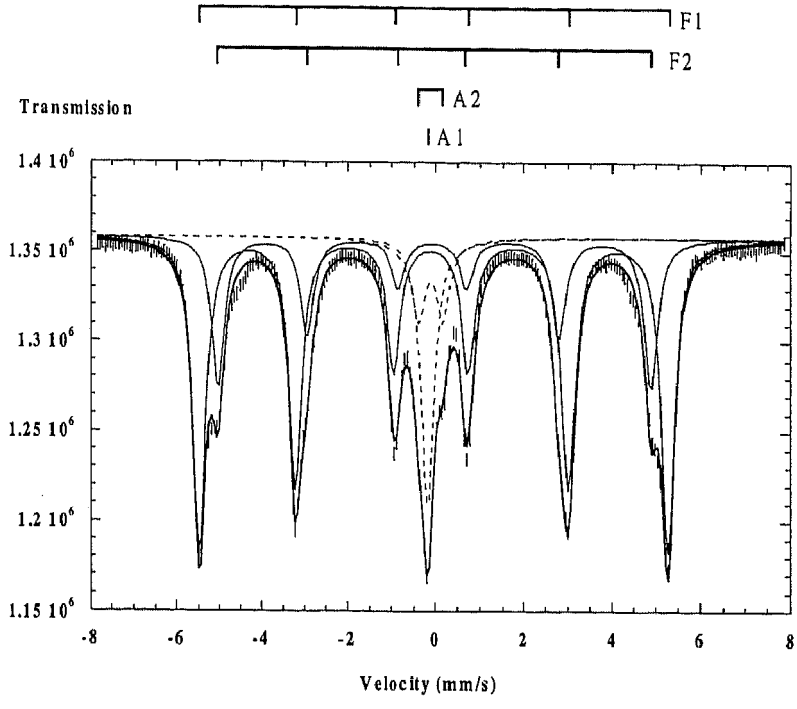

(b)

Figure 2.15: Typical Mössbauer spectra of TRIP-assisted multiphase steels. The spectra can be resolved into 2 ferromagnetic sextets (F1 and F2) and a single peak for retained paramagnetic austenite (A) (a). In the presence of high amounts of carbon rich austenite, a single peak (A1) and a doublet (A2) are needed to resolve retained austenite (b).

2.3.2.2 Estimation of the carbon content of retained austenite

The carbon content of retained austenite was estimated from the austenite lattice parameter measured from the $(220)_\gamma$ and $(311)_\gamma$ X-ray diffraction peaks using Cu-Kα radiation. During each set of measurements, the goniometer was calibrated by using peaks of a silicon standard situated close to the positions of austenite peaks. 3 measurements were carried out on each sample previously mechanically repolished and then electrolytically polished in a solution of 5% $HclO_4$ and 95% glacial acetic acid in order to remove any surface layer possibly modified by mechanical polishing. The lattice parameter was converted to carbon content using the relationship a_0 *(Å) = 3.578 + 0.033 C (wt.%)* modified as suggested by Dyson et. al. [Dyson70], in order to take into account the effect of manganese and silicon.

2.3.2.3 Monitoring of the mechanically-induced martensitic transformation of retained austenite by acoustic emission

Chapters VI and VII will focus on the mechanical stability of retained austenite and on the TRIP effect. Acoustic emission was used in order to dynamically monitor the martensitic transformation of retained austenite during tensile testing. The transducer with a bandwidth of 100-300 kHz was directly attached to the gauge length of the sample using a thin layer of high vacuum grease as coupling medium. The pre-amplifier gain was fixed at 40 dB. The continuous emission was measured using the Average Signal Level (ASL). In contrast to the Root Mean Square (RMS), the ASL is a time-average of the continuous emission, obtained by integration of the logarithmically (rather than linearly) amplified AE signal. The ASL therefore allows measurement over a wider dynamic range at the expense of resolution (which is of 1dB). The background noise level was about 7 dB for all the tests.

References

[Abe74] N. Abe, and L.H. Schwartz: *Mater. Sc. Eng.* , 1974, vol. 14, pp. 239-251

[Azev78] A.L.T. Azevedo, and E.G. da Silva: *Scripta Metall.*, 1978, vol. 12, pp. 113-117

[Chri68] B.W. Christ, and P.M. Giles: *Trans. Metall. Soc. AIME*, 1968, vol. 242, pp. 1915-1921

[Cran85] T.E. Cranshaw, B.W. Dale, and G.O. Longworth: *Mössbauer spectroscopy and its applications*, Cambridge University Press, Cambridge, 1985

[Dyson70] D.J. Dyson, and B. Holmes: *J. Iron Steel Inst.*, 1970, vol. 208, pp. 469-474

[Gen68] J.M.R. Genin, and P.A. Flinn: *Trans. Metall. Soc. AIME*, 1968, vol. 242, pp. 1419-1430

[Jatc80] C.F. Jatczak, J.A. Larson, and S.W. Shin: *Retained austenite and its measurements by X-ray diffraction*, Society for Automotive Engineers, Warrendale, PA (1980)

[Jian92] Z. Jiang, J. Lian, J. Chen: *Mater. Sc. Technol.*, 1992, vol. 8(12), pp. 1075-1081

[Ladr86] J. Ladrière, and X.J. He: *Mater. Sc. Eng.*, 1986, vol. 77, pp. 133-138

[Lepe80] F.S. LePera: *J. Metals*, 1980, vol. 32, pp. 38-39

[Maur86] T. Maurickx, R. Taillard, and J. Foct: *C. R. Acad. Sc. Paris*, 1986, vol. 303(II), pp. 41-46

[Ray96] A. Ray, and S.K. Dhua: *Mater. Charact.*, 1996, vol. 37, pp. 1-8

[Reed73] R.E. Reed-Hill, W.R. Cribb, S. Monteiro: *Metall. Trans. A*, 1973, vol. 4A, pp. 2665-2667

[Rice68] J.R. Rice: *J. Appl. Mech*, 1968, vol. 35, pp 379-386.

[Rice73] J.R. Rice, P.C. Paris, and J.G. Merkle: *Progress in Flaw Growth and Fracture Toughness Testing*, ASTM STP 536, American Society for Testing and Materials, 1973, pp. 231-245.

[Sach83] A.K. Sachdev, *Acta Metall.*, 1983, vol. 31(12), pp. 2037-2042

[Spei81a] G.R. Speich: *Fundamentals of Dual-Phase Steels*, R.A. Kot and B.L. Bramfitt ed., TMS-AIME, 1981, pp. 3-45

[Spei81b] G.R. Speich, V.A. Demarest, and R.L. Miller: *Metall. Trans. A*, 1981, vol. 12A, pp. 1419-1428

[Spei92] G.R. Speich, and K.A. Taylor: *Martensite*, G.B. Olson and W.S. Owen ed, ASM, 1992, pp. 243-276

[Vand84a] G.F. Vander Voort: *Metallography: principles and practice*, McGraw-Hill, New-York, 1984, pp. 166-172

[Vand84b] G.F. Vander Voort: *Metallography: principles and practice*, McGraw-Hill, New-York, 1984, pp. 632-655

[Vand84c] G.F. Vander Voort: *Metallography: principles and practice*, McGraw-Hill, New-York, 1984, pp. 216-217